DEVELOPMENT OF DETAILED COMPUTATIONAL FLOW MODEL OF HIGH END SERVER AND VALIDATION USING EXPERIMENTAL METHODS

by

VIJAYALAYAN PANDIYAN

Presented to the Faculty of the Graduate School of

The University of Texas at Arlington in Partial Fulfillment

of the Requirements

for the Degree of

MASTER OF SCIENCE IN MECHANICAL ENGINEERING

THE UNIVERSITY OF TEXAS AT ARLINGTON

December 2012

ACKNOWLEDGEMENTS

I would like to thank Dr. Dereje Agonafer for his continuous guidance and support over the last two years of my research and study at the University of Texas at Arlington. It has been a constant learning process for me under his expertise in terms of understanding engineering concepts and molding myself as an experienced engineer. His inspiration and motivation is beyond words.

I would like to thank Dr. Haji-Sheikh and Dr. Kent Lawrence for serving on my committee. I would also like to take the opportunity to thank Dr. Veerendra Mulay of Facebook and other Industry mentors for all their expertise and continuous support and feedback in all the projects. His industrial expertise has been really important for my research and I am very grateful to them. I am obliged to Ms. Sally Thompson who has been of immense help in assisting me in all educational matters. I also want to thank the entire EMNSPC team, especially Richard Eiland, John Fernandez, Shreyas Nagaraj, Shreyas Sampath and Harsh Patel for all the help they have provided. I would also like to acknowledge the help and support extended by all my friends and colleagues who have made my stay at UTA a memorable one.

Finally, this acknowledgement would not be complete without mentioning my parents, Mr. S Pandiyan and Mrs. Dhanalakshmi Pandiyan and my sister, Ms. Priyadharshani Pandiyan who have served as my motivation and inspiration. I am forever thankful to them for providing their support and the opportunity to pursue my dreams.

November 15, 2012

ABSTRACT

DEVELOPMENT OF DETAILED COMPUTATIONAL MODEL OF HIGH END SERVER AND VALIDATION USING EXPERIMENTAL METHODS

Vijayalayan Pandiyan, M.S.

The University of Texas at Arlington, 2013

Supervising Professor: Dereje Agonafer

The continued development of the microprocessor has led to significant increase in high frequency interconnects and power dissipation. High power devices are pushing the limits of air cooling in data center environments. Data center power consumption continues to grow at a rapid pace. In light of this increasing trend in power consumption, computer systems researchers, application designers, power and cooling engineers, and governmental bodies have all launched research efforts to improve data center energy efficiency [1].

Rack servers tend to be the main perpetrators of wasting energy and represent the largest portion of the IT energy load in a typical data center. Servers take up most of the space and drive the entire operation. The majority of servers run at or below 20% utilization most of the time, yet still draw full power during the process [2]. Energy efficiency may be achieved by improving efficiency at server level. Optimization of server requires experiment with various combinations, orientations of components to help improve the performance envelope. Experimental analyses of such trials

are both expensive and time consuming process. This gap is bridged by extensive use of CFD software which gives us the versatility and precision in virtually simulating a test setup.

The first part of the thesis will discuss the design and flow analysis of IT servers using commercially available CFD software. The CFD modeling and analysis will include the study of pressure drop and volumetric flow through the server. The servers pull in cold air through the server inlet and push the hot air through the opposite side. The detailed modeling would help us experiment with various combinations, orientations of components to obtain a highly efficient server and also to develop a simplified or compact model of the same to analyze room and rack level study.

The second part will discuss the experimental methods used to validate CFD model. The study performed in collaboration with an industrial partner and as initiation to develop simplified part library for further study.

TABLE OF CONTENTS

LIST OF ILLUSTRATIONS

Figure Page

LIST OF TABLES

NOMENCLATURE

ρ	Density (kg/m^3)
k	Thermal Conductivity (W/m-K)
$\boldsymbol{v}$	Velocity (m/s)
μ	Viscosity (N/m^2S)
ε	Kinematic Rate of Dissipation (m^2/s^3)
$\dot{m}$	Mass Flow Rate (kg/sec)
Q	Heat Load (KW)
P	Power (W)
$\dot{v}$	Volumetric Flow Rate (cfm)
p	Pressure (Pa)
T	Temperature (K)
C_P	Specific Heat Capacity (J/kg-k)
R_e	Reynolds Number
l	Characteristic Length (m)

CHAPTER 1

INTRODUCTION

1.1 Data Center: An Introduction

The rise in cloud computing, virtualization and data storage require high performance data centers. Data centers are continuing to expand day by day in terms of size, technology, power, density etc. Adding to this is the cost of energy to cool these servers and the maintenance cost required to prevent them from failure. Power, cooling and application Engineers are trying to improve the data center efficiency by improving the server design. Data center can consume 100 to 200 times the power consumed by a standard office [2]. The trend is expected to rise further every year.

These data centers house several servers, a large amount of power is utilized and a tremendous amount of heat is generated. The servers along with other electronic components generate a large amount of heat and hence it is crucial to ensure that the air temperature inside the containerized data center is within the prescribed limits in order to avoid hot spots. Hot spot formation and thermal stresses can lead to equipment failure, short term reliability etc. Several factors such as ambient temperature, humidity, location play an important role as thermal conditions are based on ambient conditions as well as conditions inside the data center. Also, reduction in chip size and high chip utilization rates has led to an increase in heat density of chips at a rapid rate. Therefore, in order to maintain optimum performance of these devices, thermal management is very important at the device, board, and rack and room level.

The regulations are being updated every year trying to maximize the conditions to obtain an optimum data center performance. But, still there is a need for improving the efficiency at server level which in turn would improve the data center efficiency by a greater extent.

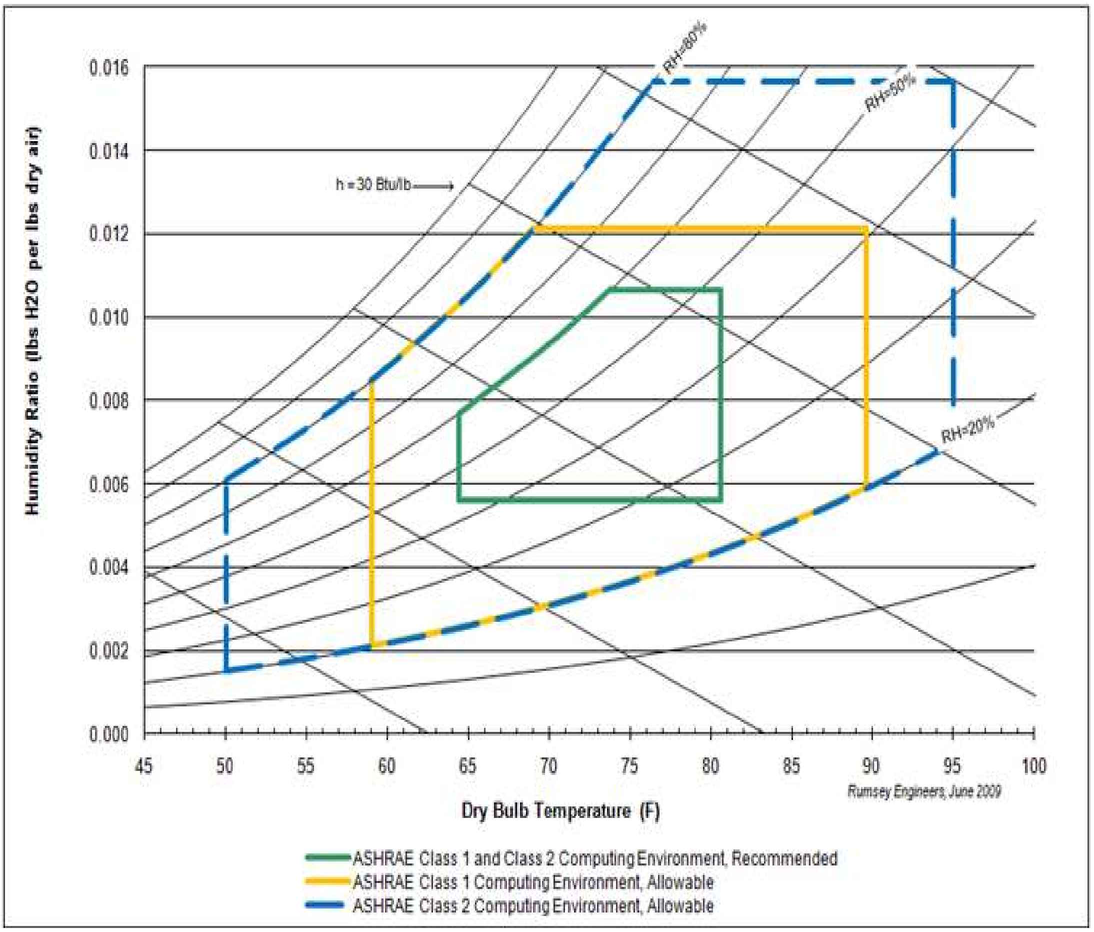

Figure 1 ASHRAE recommended operating conditions for data centers [3]

The need for speed and efficiency has caused rapid change in electronics technology. Engineers have launched efforts to find alternate viable options to and novel approaches to removing increasingly large amounts of heat energy from a smaller space. This should be performed carefully without compromising the existing reliability and functionality of the servers.

Figure 2 Graphical representation of a data center [4]

1.2 Types of Server Chassis

The servers nowadays are designed to be efficient, fast and compact as well. Reducing the server foot print reduces data center space. Servers are classified based on their application. Platform servers, Application servers, mail servers, proxy servers, web servers and communication servers are few of the types. The servers are also classified in terms of the chassis as Blade servers and Rack Mount servers. The blade servers are servers with modular design optimized to minimize the use of physical space and power [5]. These servers are placed in an enclosure which can hold multiple servers and provide other non-computing related operations like cooling, power and networking.

Figure 3 IBM HS20 blade servers [5]

Blade servers are cost-efficient and slim, housed inside a chassis, which is also called a cabinet. The blade servers within the same chassis are connected using a bus wiring system. The blade servers share a network connection, power supply and cooling systems. Blade servers are considered to have more common cooling issues because rack-mounted servers each have their own individual cooling systems [6].

Figure 4 HP blade system C7000 blade enclosure [5]

The rack mount servers are contained in cases measuring standard sizes termed as 1 U servers (1U=1.75”), which are mounted in a rack inside a cabinet. The rack servers a have individual cooling and can operate individually. Other advantage of using rack servers is the capability of using servers from different manufactures.

Figure 5 Open compute server [7]

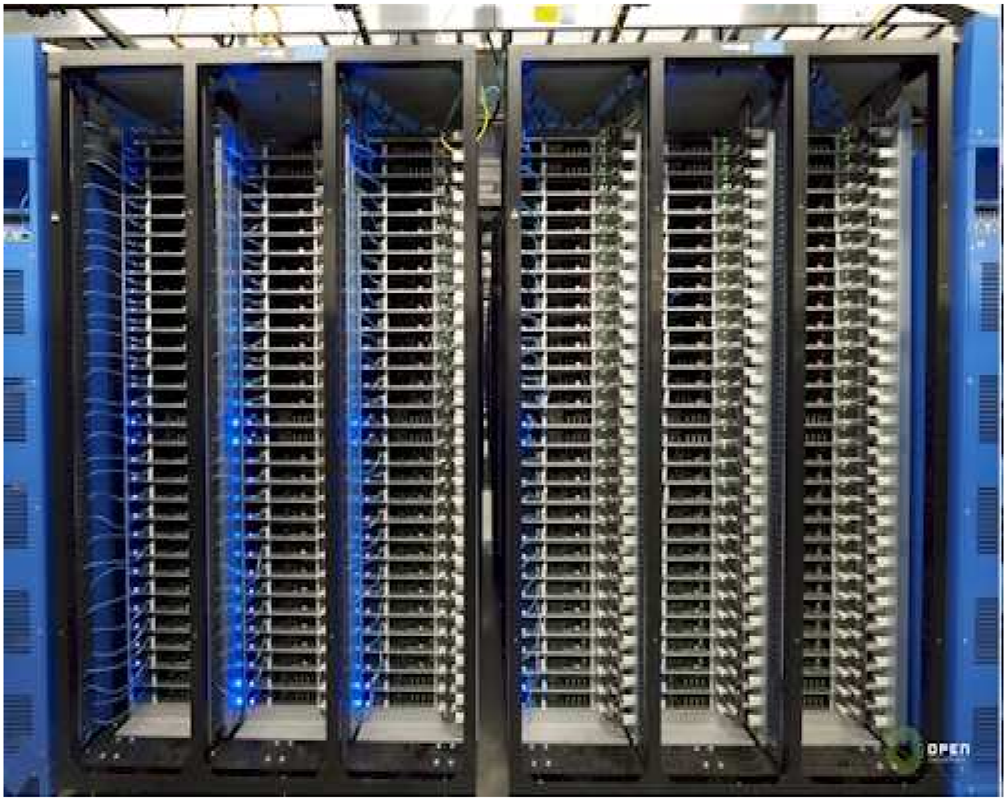

Figure 6 Open compute triplet rack [8]

1.3 Need for Cooling

Server downtime is a very important term used in data center industry. Server downtime is the time during which the server is unusable. Server downtime may be caused due to various reasons like memory overload, overloaded processors etc. All the mentioned reasons would impact the cooling required by the server. The company's data center is often very critical and has to be well protected. The sever chips are the main source of heat generation and it is very important to keep the chips within the operating temperature range. Servers generate a large amount of heat in relatively small foot print. The power used by server is dissipated as heat into the ambient. The power of a processor can largely depend on the amount of heat removed.

The heat dissipated is largely non-uniform and fluctuates frequently. Non uniformity in power may be caused due to various reasons. For example, heat load variation may occur with time due to addition of workload or due to the mix of hardware. Data center accommodates components sensitive to heat and humidity. Large number of failures has found to occur at chip level. As we know, the server performance is proportional to the temperature at which the chip operates and it also affects the shelf life of the chip considerably.

The air flow through server chassis is key aspect affecting the cooling efficiency of a server as the main mode of heat transfer occurring in a server is through convection and conduction. Conduction happens at chip level and convection occurs at a cabinet level which is of a different scale when compared to chip level. Components like heat sinks, fans are employed to enhance the process of convection. Alternate cooling solutions like heat pipes, vapor chamber heat sinks may be utilized but, its efficiency depends on the availability of air flow through the server. While designing care should be taken to ensure proper flow through the server is available to satisfy the varying heat load. Care should be taken while providing vents to aid the server cooling process.

1.4 Need for CFD Modeling

As discussed in the previous section, one can understand the importance of air flow through the server. The factor affecting the flow through the server is pressure drop. To push air from a point to another, a potential difference is required. This potential difference is the pressure drop. It is appropriate to determine the pressure drop required to drive the required volume of air through the server. A CFD model helps us determining these parameters thereby giving us a prediction about the capability of the design. These predictions may be determined experimentally. But, experimental testing consumes time and is expensive. This gap is bridged by extensive use of CFD software which gives us the versatility and precision in virtually simulating a test setup. Optimization of servers requires experiments with various combinations, orientations of components and helps to improve the performance envelope. It is easier to study the effects of the changes virtually than by experimental testing. The focus of this study is to develop a detailed flow model of the server, which can be used for thermal analysis and also may be used to develop a compact/simplified model for conducting studies at rack and room level.

CHAPTER 2

SERVER DESCRIPTION

2.1 Server Description

The pressure drop across a server and the volumetric flow rate through the server can determined either by experimental testing or by using CFD modeling. Though experimental may be time consuming and expensive, they give us exact results when compared to CFD. It is highly unlikely to develop a model which accounts for all the key aspects of the geometry and gives accurate result as an experimental test. Certain details like the curvature of components, fans have to be simplified in order to reduce the complexity of the CFD model. Hence we try to develop a detailed model which may be not as accurate as the physical model but, represents the key features of the physical model.

The experimental results are used to validate the detailed CFD model with a permissible deviation range from experimental results. The components may share approximately same details both experimentally and virtually but, they need not perform the same way as in reality. Thus validation of CFD model with experimental results is necessary to ensure the predicted performance in comparison with reality. This also ensures the reliability in behavior of simplified models obtained using the validated detailed model.

The server under study is from open compute project and has a dual Intel Xeon® 5500 or Intel Xeon® 5600 socket motherboard with 18 DIMM slots constituting a 1.5U server [7]. This study indicates the need for detailed model to obtain an accurate CFD model. System resistance and flow rate were determined using CFD and compared with experimental data.

This chapter will describe the experimental methods and tools utilized. These experiments were also used to determine components pressure drop, fan curves and power curves [9].

2.1.1 Motherboard

The server under investigation is a is a dual Intel Xeon® 5500 or Intel Xeon® 5600 socket motherboard based server with 18 DIMM slots. The motherboard uses Intel CPUs with a TDP (thermal design power) up to 95W. It constitutes three DDR3 RDIMMs per channel per CPU and hold up to 9 RDIMMs per CPU. The motherboard also consists of Intel**®** 5500 I/O Hub chipset. They operate on 12.5 VDC supply delivered by the power supply unit. The motherboard powers six hard drives connected using traditional 4-pin floppy connector.

Figure 7 Intel Based Open compute server [10]

2.1.2 Server Chassis

The chassis is 2.6 inches tall - that's 1.5U in rack–form factor. It is taller than 1U chassis which allows the use of taller heat sinks and larger diameter fans. The server chassis is made with 1.2mm zinc-plated corrosion resistant steel with neatly integrated cables and 4 rear mounted fans [11]. The server is equipped with snap plungers to reduce the amount of fasteners to hold components. The below table illustrates the thermal specification as found in the open compute project website.

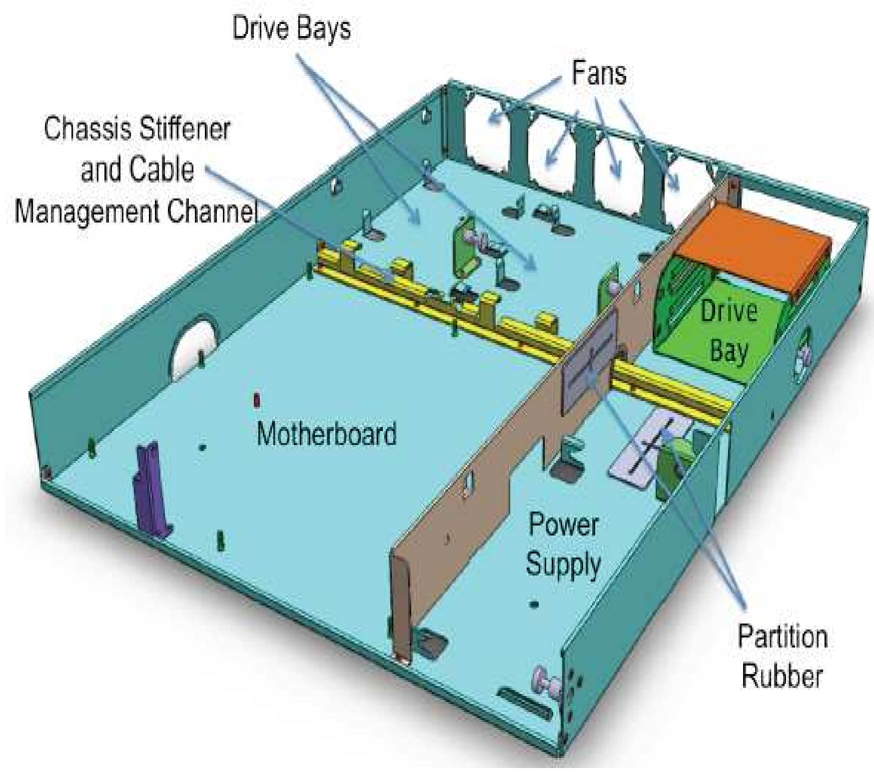

Figure 8 Graphical representation of the server chassis [11]

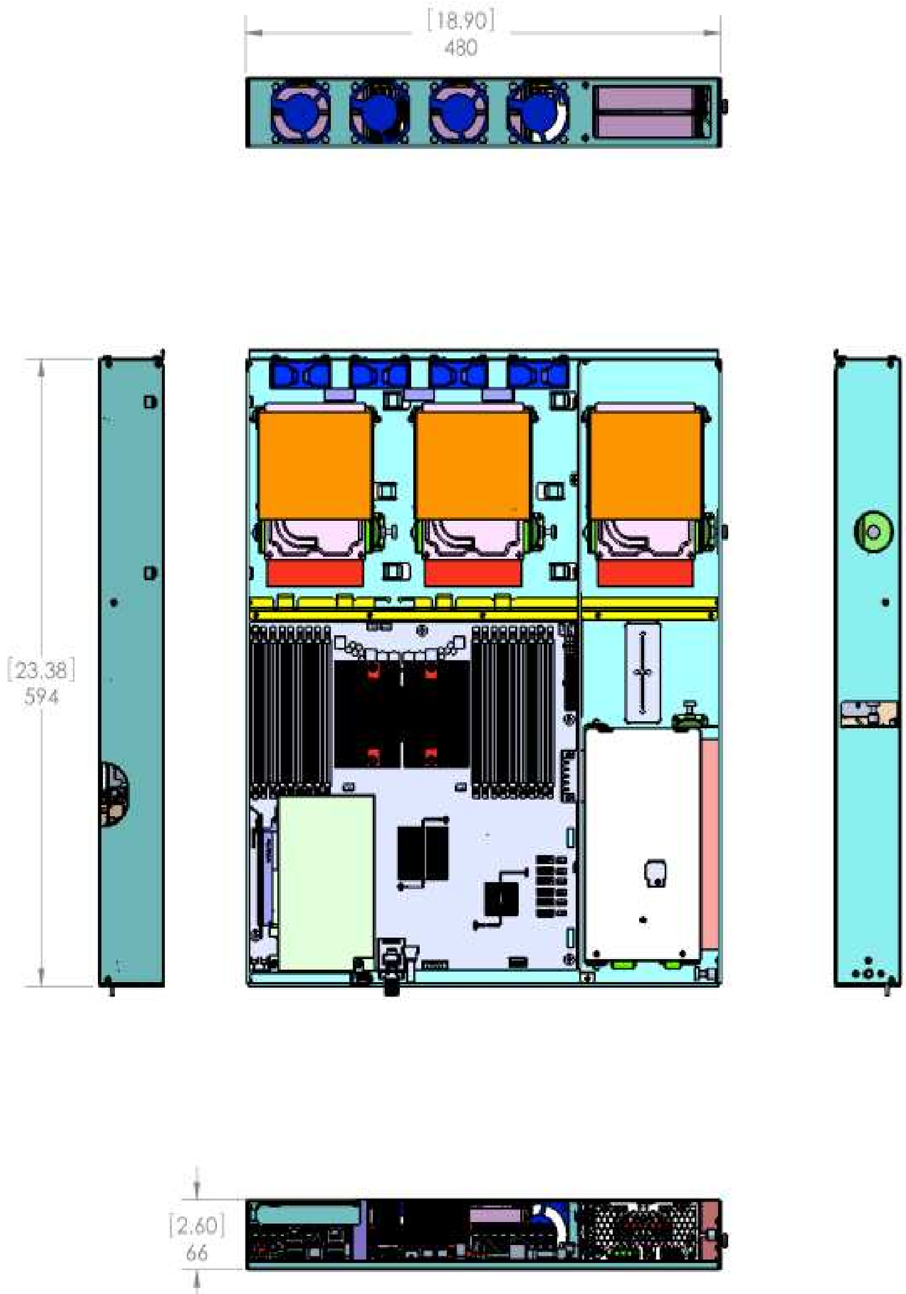

Figure 9 Graphical representation of the chassis dimensions (All dimensions are in [inches] and mm) [11]

Table 1 Thermal specifications at server level [11]

	Server Level	Rack Level
Loading	Idle to 100%	
Inlet temperature	65°F to 95°F (35°C)	65°F to 85°F
Pressure drop within system	Intel motherboard: 0.005 to 0.24" H2O AMD motherboard: 0.004 to 0.22" H2O	
Total CFM requirement for above pressure levels	Intel: 12 to 103 CFM AMD: 14 to 106 CFM	Intel: 864 to 7416 CFM AMD: 252 to 1908 CFM Total: 1116 to 9324 CFM*
Fan RPM	Varies from 1120 to 7600 rpm with 10% tolerance.	
Humidity**	Approximately 30 - 65%	
Altitude	1000m (~ 3300ft)	
Dewpoint**		41.9°F minimum

2.1.3 Server Fans

The server is cooled with the help of four Delta 60x60x25.4mm fans placed at the rear end of the server. The fans are controlled by the motherboard based on the core temperature using a fan speed control algorithm. The fans pull required air through the server system.

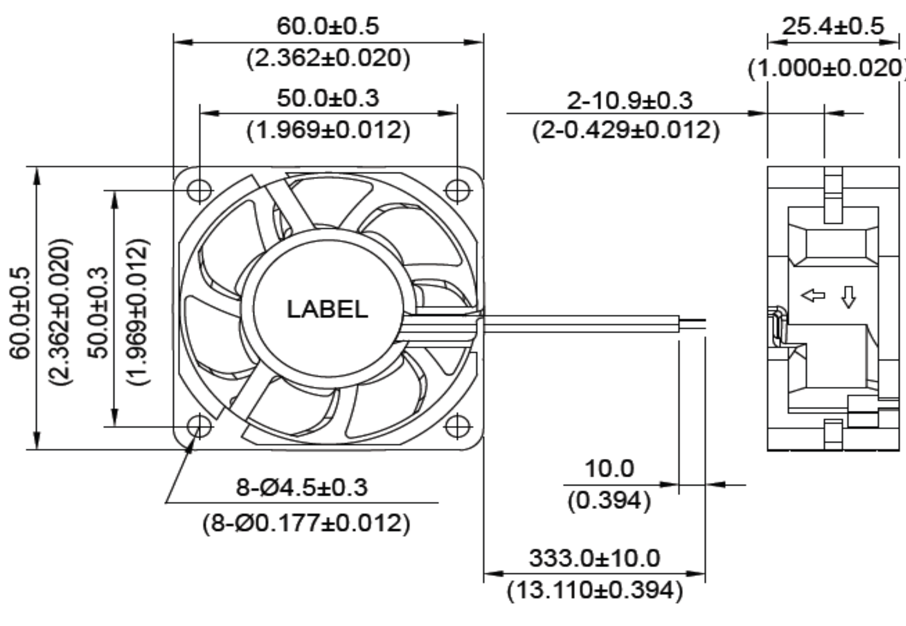

Figure 10 Fan dimensions [unit: mm/ (inches)] [12]

The fans used are four pin fans which are controlled u sing a PWM signal. As the PWM signal is increased or decreased, the fan speeds vary correspondingly. Fans have a maximum air flow of 43.30CFM at free flow condition and maximum speed of 9000 R.P.M. Fans operates 0n 12VDC consuming 5.64W power at maximum speed. It has a maximum static pressure of 0.763 in/H_2O at no flow condition.

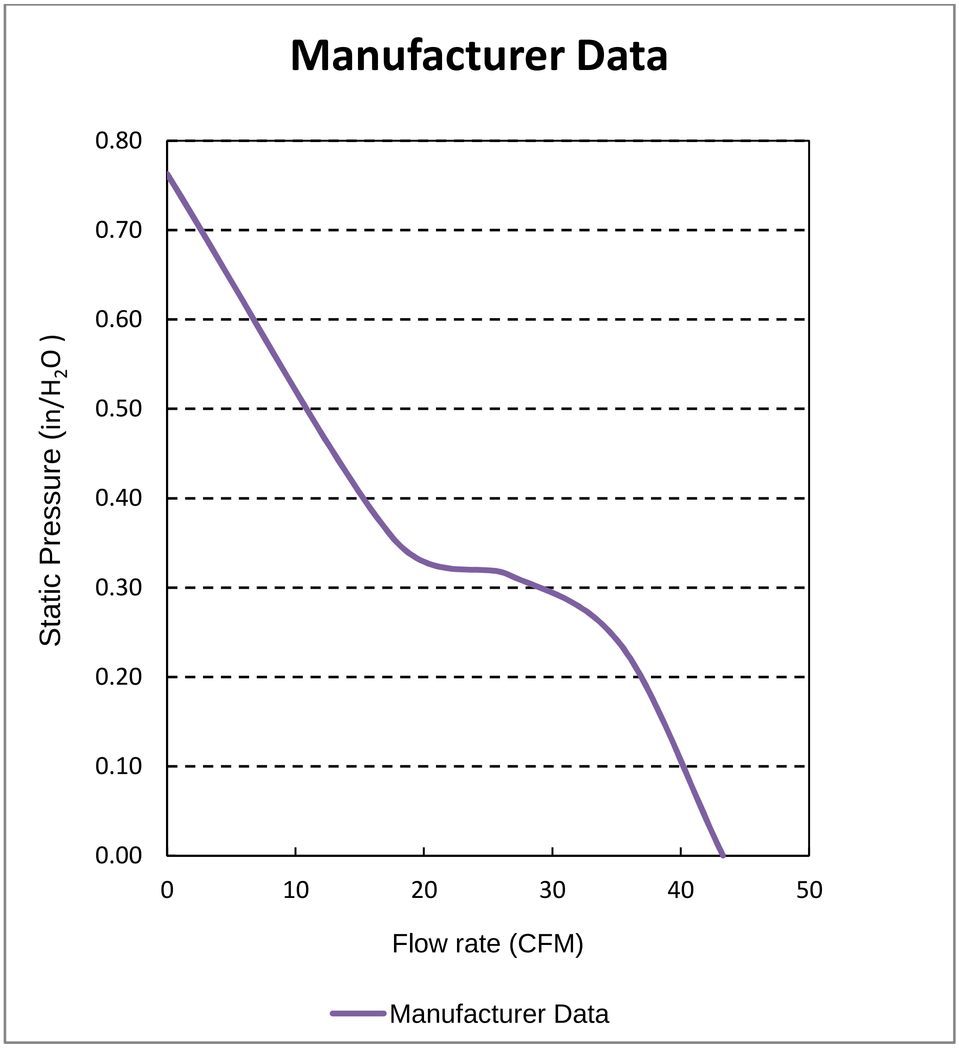

Figure 11 Manufacturers Fan Curve data [12]

2.1.4 Heat Sinks

Heat sinks are components used to cool heat generating devices by dissipating heat to the ambient air by convection heat transfer. The server under study employs two straight fin aluminum heat sinks, one for each processor to keep them within the operating temperature range. The heat sink is mounted using screws. The mounting device consists of a back plate and receptacles for screws.

2.1.5 Power Supply Unit

The power supply unit used in the server is a 450W power supply can operate on either 277VAC source or 48VDC. The nominal output voltage is 12.5VDC and is powered directly by PSU output. The power supply is self-cooled using a separate internal fan. The air is pulled from the front end of the powers supply. The fan is a Delta AFB series 4-pin fan measuring 60x60x25.4 in dimension.

Similar to the server fans, The PSU fans are controlled by the motherboard based on the inlet air temperature. The PSU fan operates at minimum PWM of 30% irrespective of cooling conditions to prevent the formation of hotspots. The fan speed don not vary with server loading. The fan's L10 lifespan is at least 50,000 hours at 45℃ inlet air temperature and full speed [13].

Table 2 Efficiency of Power supply unit at various loading conditions [13]

Efficiency (%)	Load (%)
>90	20
>94	50
>91	100

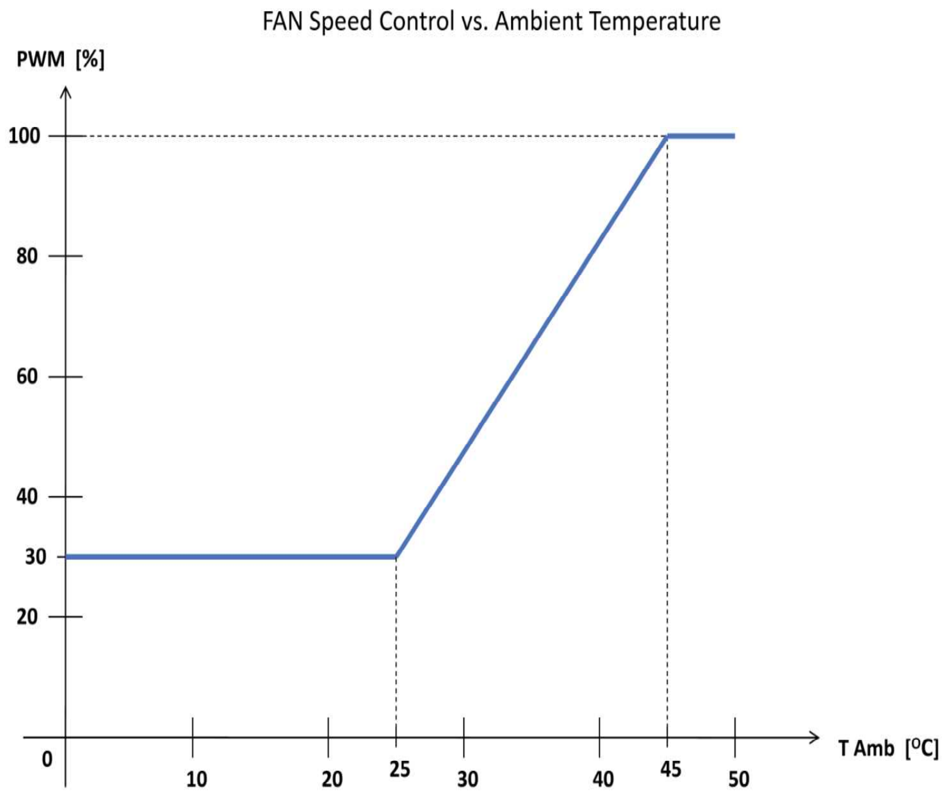

Figure 12 PSU fan speed control vs Inlet temperature [13]

CHAPTER 3

PARAMETERS TO VALIDATE A CFD FLOW MODEL

3.1 Static Pressure Drop and Fan Curves

In order to validate a CFD model, determining static pressure drop across the server experimental is a key parameter. Air flow through any system or enclosure is based on the resistance the system offers to the flow causing a drop in pressure across the system. The pressure decreases from one point to another point downstream due to the frictional force on a fluid as it flows through the server components. The pressure drop is influenced by the fluid velocity and viscosity of the fluid. If the fluid is at high velocity, there is large pressure drop across the system when compared to the same fluid traveling through the system at lower velocity. Hence it is very important to determine the flow characteristics of components in the server.

Similarly, it is important to determine the fan performance curve as it determines the fans performance at different static pressure conditions. A fan curves give us an overview on the amount of airflow it can deliver at various static pressure across the system. Each fan has its own fan performance curves. Using system impedance and fan curve, we can determine the optimum operating point by imposing both the curves and find the intersecting point.

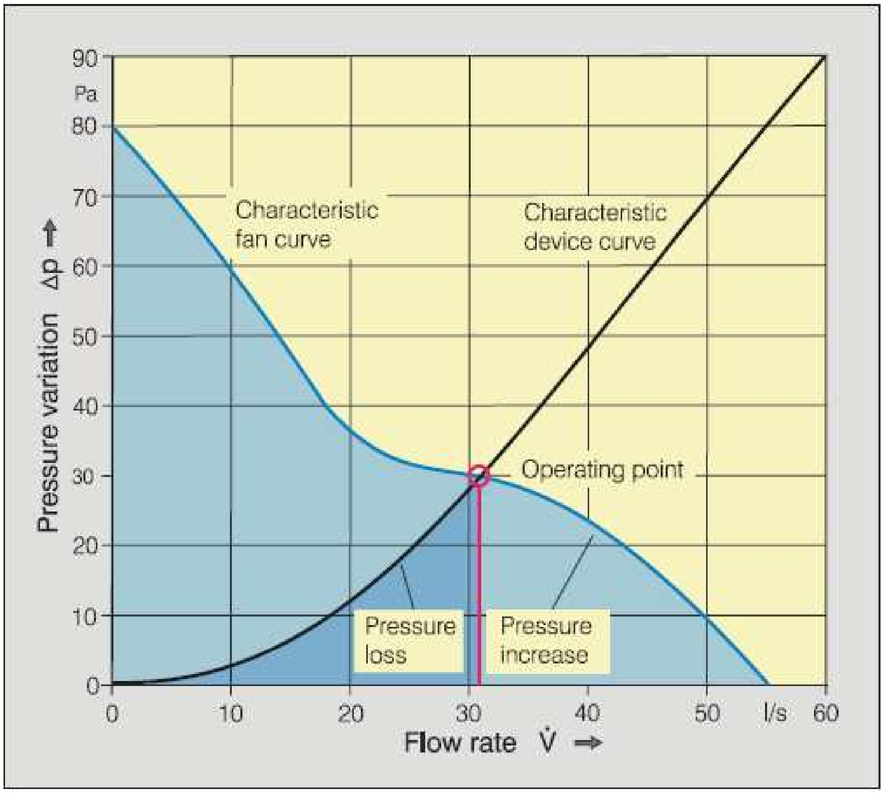

Figure 13 System impedance curve and fan curve [14]

3.2 Airflow Rate

Once we determine the pressure drop, we have to experimentally determine the volumetric flow rate through the server at various fan speeds. The fans are controlled by the motherboard based on the core temperatures of the CPU. It is important to determine the volumetric flow rate as to have knowledge on the amount of air available to cool the server. As the CPU temperature increases, the fan speed increases which in turn increases the volumetric flow rate through the server to cool the CPU temperature and maintain it within the operating range.

CHAPTER 4

EXPERIMENTAL METHODS AND TOOLS

4.1 Airflow Test Bench

The volume of air required to cool a system may be calculated accurately if the heat dissipated and temperature difference between inlet and outlet is known. But the pressure required in moving the required volume of air through server is not easy to calculate. This is important as the required fan has to be selected for pushing or pulling the air through the system.

Airflow test bench is used to determine the static pressure drop across the system and volumetric flow rate. It is also used to determine fan performance curves and system impedance of components. The airflow bench used was manufactured by Airflow Measurement systems and is designed in accordance with AMCA 210-99. The test chamber uses multiple nozzle diameters to cover a wide range of airflow rate. The chamber consists of pressure taps connected directly to the chamber to measure the static pressure of the system under study. The pressure taps also measure the differential pressure across the nozzle to determine the flow rate through the nozzle.

Figure 14 Airflow test bench

4.1.1 Airflow Test Bench Setup

The airflow test bench has two chambers separated by a nozzle plate in between. The pressure taps connected to the chamber is connected to a pressure transducer which has differential pressure range from 0 to 5 in. WC. The transducers use a stainless steel micro-tig welded sensor [15]. The tensioned diaphragm and insulated electrode are placed closed to each other to form a variable capacitor. Positive pressure moves the diaphragm towards the electrode causing the capacitance to increase and vice versa. The capacitance change is converted to a voltage signal and is converted to a pressure value using software.

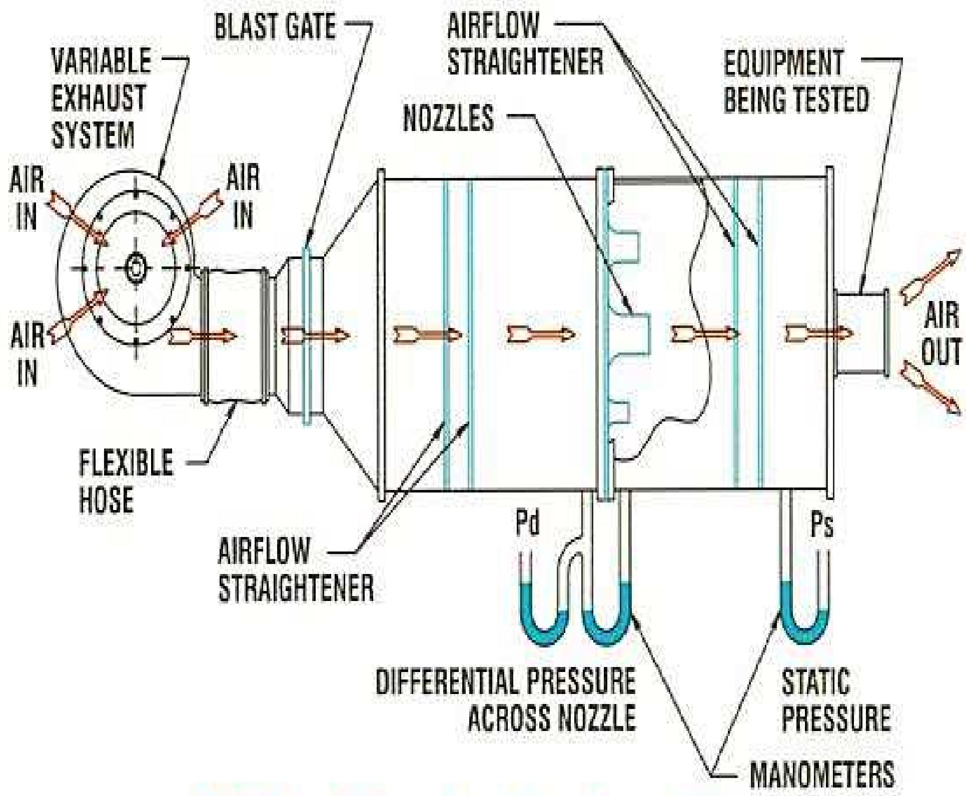

Figure 15 Airflow test bench setup [16]

The nozzle selected based on the required flow rate from the nozzle selection chart. The nozzles are sized and positioned on the plate in such a way that they may be used in parallel to attain higher flow rates. Each nozzle is provided with stoppers to shut off flow through it when not in use. The minimum flow range achieved using this airflow test bench is 3CFM.For flow rates below 3CFM may be achieved using smaller nozzles.

Figure 16 Pressure transducers

According to the manufacturer to have a better resolution, the maximum flow should be near to +3 in WC range in differential pressure. In case the flow range is unknown, verify the free delivery by selecting 2 in diameter nozzle. If the differential pressure is below 1 inches WC, then select a nozzle with smaller diameter and select a nozzle with higher diameter if the differential pressure exceeds 4 inches WC. The airflow chamber utilizes a counter blower which is controlled by a speed controller. By varying the frequency in the speed controller box, we can vary the blower speed. The air is delivered into the chamber using a flexible hose. The amount of air flowing through the chamber can also be regulated using blast gate, a sliding gate valve found at the end of the chamber.

Figure 17 Nozzle plate front side

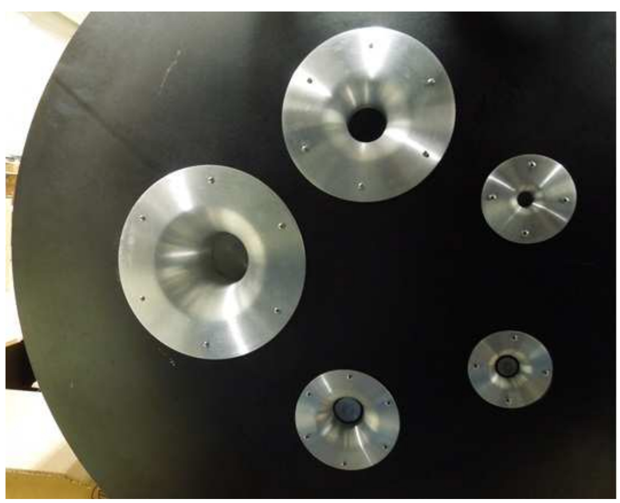

Figure 18 Nozzle plate back side

The test bench is assembly of various parts and leakage of air can be an important issue. Any leakage in the system would lead to false values. Inflatable seals are used on each side of the nozzle plate and at the front plate. These seals are inflated using compressed air to a maximum pressure of 30 PSIG. The pressure can be controlled using a regulator connected to the chamber seals.

4.2 Fan Speed Control

Fan speeds as mentioned earlier are controlled by the motherboard using PWM signal. To measure the fan performance, fan speed control has to be replicated to attain ranges from no flow to free flow. Fans used in server are 4 wire fans. A 4 wire fan consists of power, ground, sense and control wires. Sense wire reads the fan speed like a tachometer. Based on the tachometer reading, fan speed algorithm and the CPU temperature sensor reading, the motherboard decided to either increase or decrease PWM signal through the control wire. Pulse-width modulation (PWM) is used to control motor by using a succession of “on-off” pulse. By varying the width, the power to the motor is regulated. The width of the PWM signal or the portion of ‘on’ time to the total time period is called a duty cycle. The width of the on-pulse sets the duty cycle and thus the average voltage supplied to the fan motor. When we increase the duty cycle, the “on” cycle width is increased thus increasing the fan speed. Duty cycle is represented in percentage.

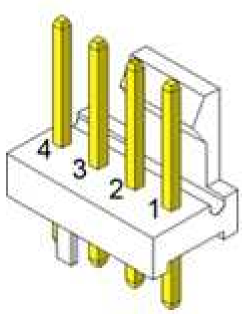

Pin	Name	Color
1	GND	black
2	+12VDC	yellow
3	Sense	green
4	Control	blue

Figure 19 4-pin fan configuration

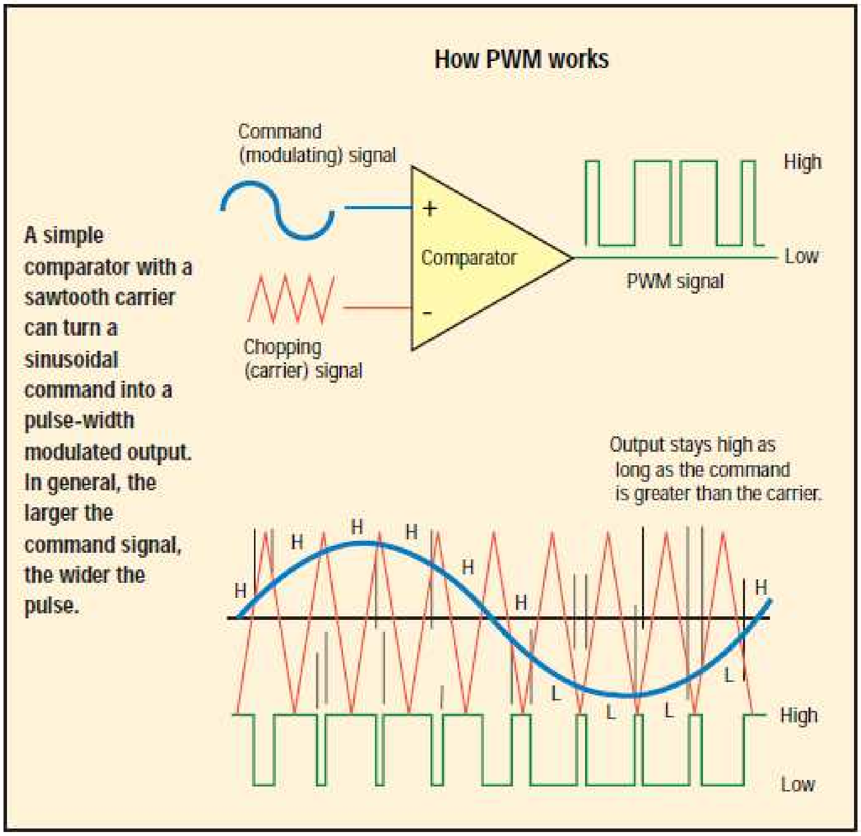

Figure 20 PWM working diagram [17]

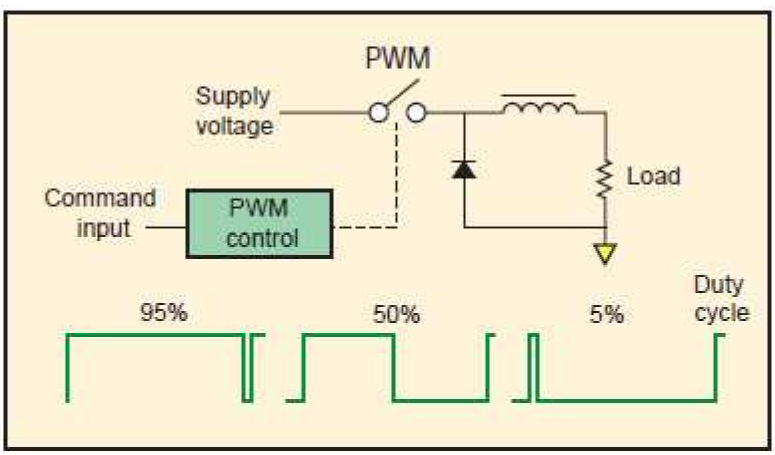

Figure 21 Duty cycle illustration [17]

This setup is replicated using a DC power supply and a function generator. The DC power supply is power source which is connected to the ground and power wire of the fan. A function generator is connected to the control wire to regulate the power to the fan motor using PWM signals. By connecting a tachometer to the sense wire, we can determine the fan speed corresponding to the specified duty cycle.

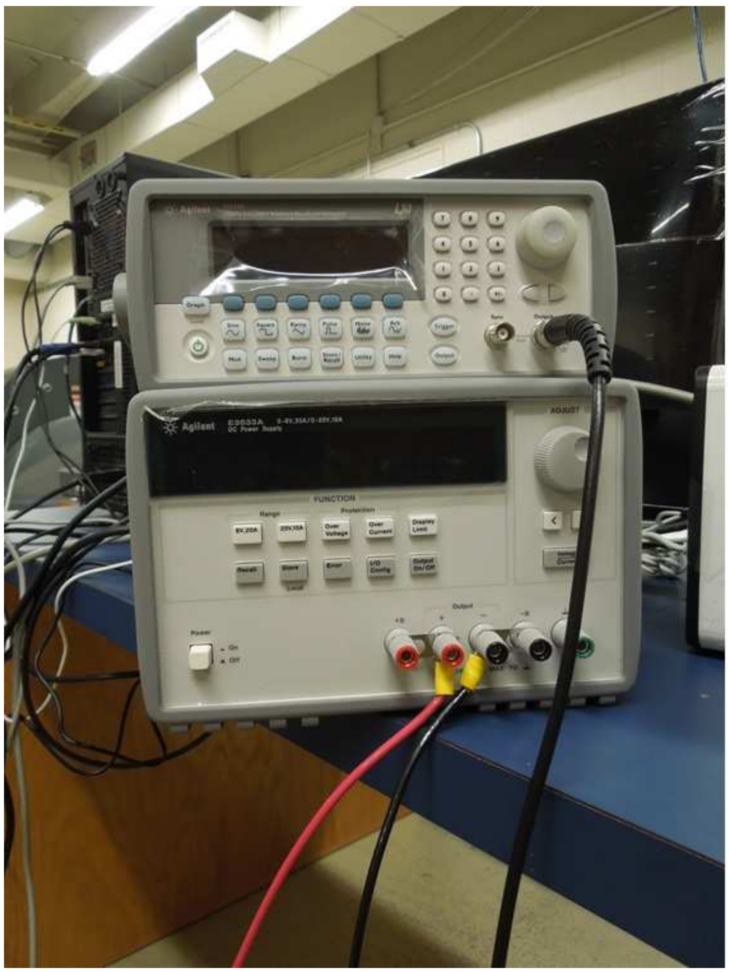

Figure 22 Function generator and DC power supply

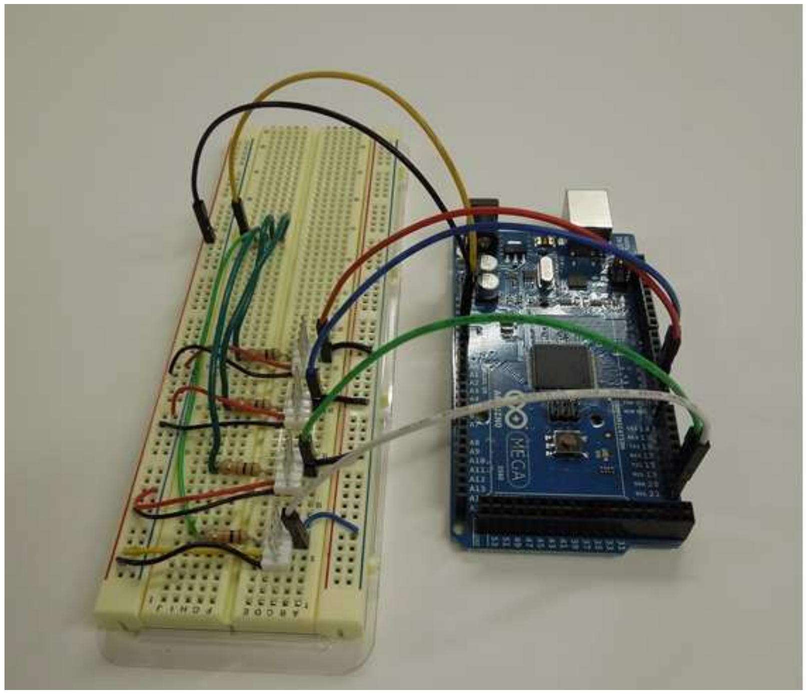

Figure 23 Arduino and Bread board connection circuit

4.3 Static Pressure Drop Measurement

The server inlet was placed on the outlet of the airflow bench. The server inlet was pushed slightly inside the chamber to avoid any loses. The setup was sealed using a tacky tapes to avoid air loss. All possible leaks have to be sealed. The fans have to be removed from the server to avoid additional resistance. All holes and vents on the server chassis have to sealed or closed except fan vents.

The airflow bench was setup to push air through the chamber. The flexible hose was connected to the blower outlet and the other side of the hose was connected to chamber inlet. The blast gate was completely open. The nozzle array was positioned towards the flow downstream. The nozzle is selected based on the flow rate required. The stopper was removed from the required nozzle alone. The tubes from the chamber before and after the nozzle array plate were connected to the high and low ports of the pressure transducer. The difference in pressure before and after the nozzle is the differential pressure. Differential pressure was used to determine the velocity of air through the nozzle. The tube near the server inlet was connected to high port of the pressure transducer and low port was left open to the atmospheric pressure. The difference is the static pressure of the system. The frequency of the blower is varied and the static pressure values are recorded for different flow rates. The static pressure values are plotted against flow rates giving us the system curve of the server.

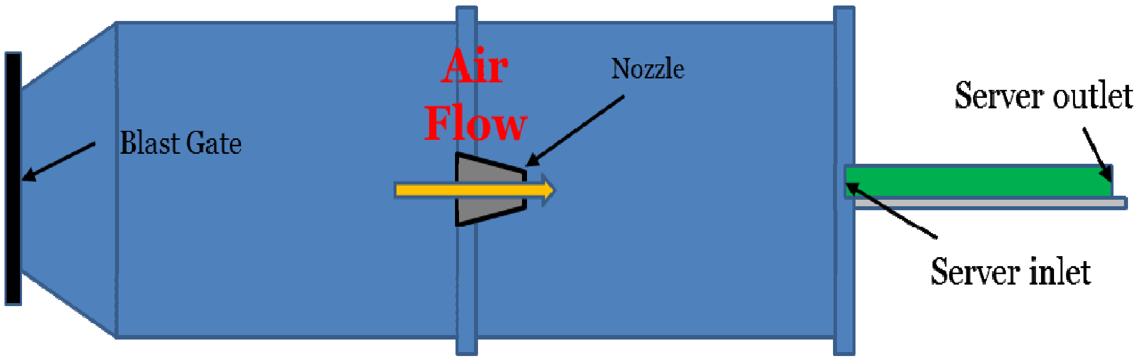

Figure 24 A representation of the experimental setup

Similar procedure was followed for three different server configurations.1 complete server, 2 server without fans, 3 server without fans and PSU. This was done to study the flow characteristics for different server configurations.

Figure 25 Server setup without fan and PSU

The inlet and outlet side of the PSU was completely closed to avoid leakage of air through it. In this study, the server was considered as two units, motherboard part and powers supply unit part which do not influence flow in each other. As explained earlier, the motherboard part has four fans running in parallel to address its cooling requirements and PSU has its own self powered cooling fan. The server load only control the fans powered by the motherboard and the PSU fan does not vary with the CPU load. The PSU fan speeds vary only with variation in the inlet air. The motherboard and PSU part has been separated by a wall. Moreover, the power supply unit by itself is a sub chassis with numerous components inside an enclosure and hence the PSU was treated as a separate unit. The static pressure drop for PSU was carried out separately to validate the PSU CFD model. The fan was removed and similar procedure as described above was followed for PSU static pressure drop measurement.

Figure 26 PSU static pressure drop measurement experimental setup

CHAPTER 5

CFD (COMPUTATIONAL FLUID DYNAMICS) ANALYSIS

5.1 Introduction to CFD

CFD (Computational fluid dynamics) is a branch of fluid mechanics which deals with the numerical simulation and analysis of fluid flow, heat transfer characteristics and pressure characteristics. Computational fluid dynamics uses numerical methods to predict, simulate and analyze distribution of velocity, pressure, temperature and other variables throughout the calculation domain. The results can be used to analyze the design and helps to optimize the design process and products [18]. Computers are used to perform the calculations required to simulate the fluid interactions with surfaces based on the boundary conditions. CFD analysis was primarily used in aircraft and automobile industry. But, it is now widely used for various applications such as data center industries, systems with high heat loads, telecommunication industry, and several more.

CFD results are directly analogous to wind tunnel results obtained in laboratory –they both represent sets of data for give flow configurations at different Reynolds numbers [19]. CFD acts as a link between pure theory and pure experiment by helping us clearly understand the results of theory and experiment. CFDF is also a design tool. The advantage of using these numerical methods is that the problem can be discretized based on a set of numerical parameters and solved. It is less expensive when compared to conducting an experiment for every change we make to optimize the design. When compared to conducting an experiment, CFD is very fast as we can simulate many cases in specific time period. The simulation tools offer a repository of features that can be used such as grid generation, mesh sensitivity analysis and several other features. A numerical prediction is used for the generation of a mathematical model which represents the physical domain of interest to be solved and analyzed. In this particular case, the study involves the system level equipment such as the server chassis, the electronics and other equipment like the power supply unit, hard disk drive etc. that are housed in them.

With the increasing application of CFD in various fields, need for high speed computing has also increased rapidly. Earlier serial machines were used for high speed computing, but now different computer architectures are being used to expedite the computation process. The two new architectures primarily used are vector processing and parallel processing [19].

5.2 Governing Equations

Computational fluid dynamic codes are based on Navier-Stokes equations. The numerical solution for heat transfer and fluid flow based problems is obtained by solving a series of three differential equations. These three differential equations are the conservation of mass, conservation of momentum and conservation of energy. They are very commonly known as the governing differential equations [20].

For a generalized case, the conservation of mass is given by:

$$\frac{\partial \rho}{\partial x} + \nabla.(\rho u) = 0$$

The conservation of momentum for a generalized case is given by:

$$\frac{\partial}{\partial t}(\rho u) + \nabla.(\rho u u) = \nabla.(\mu grad u) - \frac{\partial p}{\partial x} + B_x + V_X$$

The conservation of energy for a steady low velocity flow is given by:

$$\nabla.(\rho u h) = \nabla.(k grad T) + S_h$$

5.3 Global Computational Domain

In a general flow field, when we consider a closed volume within a finite region of flow. This is closed volume is defined as a control volume. The computational domain or the solution domain is the region or space within the closed volume in which the governing differential equations are solved. The control volume may be fixed in space or may be moving with the fluid

[19]. The solutions to these equations are obtained by fixing the boundary conditions for the solution domain. The boundary conditions for most computational problems include the external ambient temperature, velocity, pressure, mass flow at inlet and outlet, fluid viscosity, thermal conductivity, specific heat and other environmental conditions. It depends on the type of heat transfer such as conduction or convection and also any radiation factors. In addition, the conditions at the domain wall also need to be specified whether they are open, closed (adiabatic) or symmetrical in nature.

The major steps in CFD is defining the geometry of the problem, dividing the volume into discrete cells also called as meshing, applying boundary conditions and finally solving the governing equations. The discretization is important as it converts the differential equations into algebraic equations. There are many ways to discretize a problem and the primary methods are Finite Difference Method, Finite Element Method and Finite Volume method. Finite Element Method is widely used in analysis of solid structures, but can also be used to analyze fluids. In this method, the geometry is divided into small elements and solved in relation with each other. Finite Volume Method where the governing equations are integrated around the mesh elements whose volumes are considered for the solution and Finite Difference Method where the differential terms are discretized into series of grid points. The finite difference method becomes difficult to use when the coefficients involved in the equation are discontinuous [21].

The computational fluid dynamics code considered for the numerical analysis in 6SigmaET® [22] is the finite volume method where the solution domain is discretized into control volume regions. Thus, the governing equations are solved by integrating over the control volume and applying divergence theorem. Considering the volume of mesh elements and the variables to be calculated are located at the centroid of the finite volume.

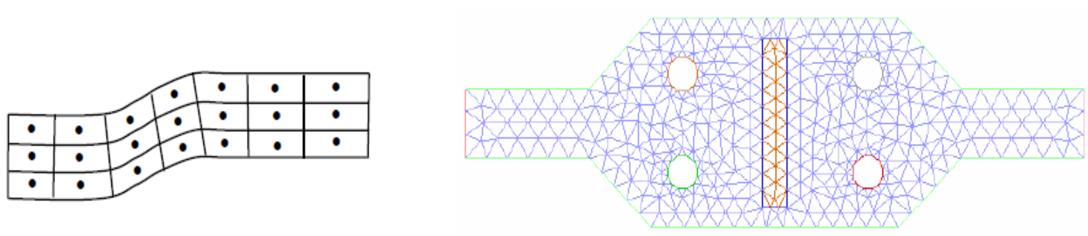

Figure 27 Graphical Representation of discretization by FVM [23]

FVM is not limited by cell shape. It may be used on arbitrary geometries which is a primary reason to use finite volume method for solving the governing equations namely conservation of mass, conservation of momentum and conservation of energy than the other computational methods. The FVM is locally conservative as it is based on a “balance” approach [21]. In FVM, the solution domain is divided into finite control volumes by a grid. The grid defines the boundary conditions [23].

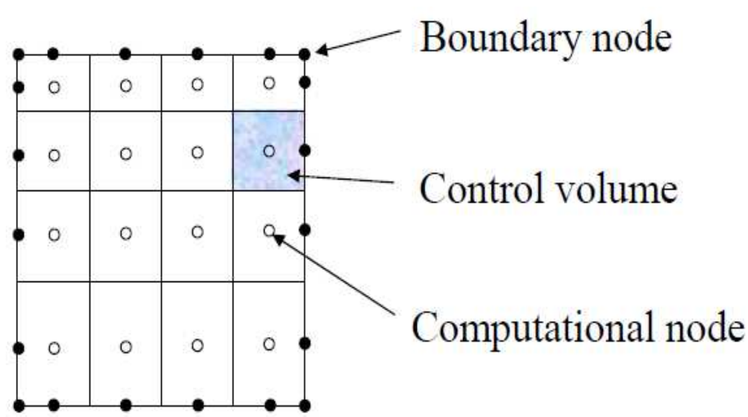

Figure 28 Graphical Representation of a 2 Dimensional Grid [23]

A series of algebraic equations are used for discretizing the results such that each of them relates a variable’s value in a cell to its value in the nearest neighboring cell. As an example, the variable for velocity “V” can be calculated using the following algebraic equation:

$$\boldsymbol{T} = \frac{\boldsymbol{C_0V_0 + C_1V_1 + C_2V_2 + C_3V_3 + \ldots C_nT_n + S}}{\boldsymbol{C_0 + C_1 + C_2 + C_3 + C_n}}$$

Where $\boldsymbol{V_0}$ represents the velocity value within the initial cell; $\boldsymbol{V_1}, \boldsymbol{V}, \boldsymbol{V_3}, \ldots \boldsymbol{V_n}$ are the velocity values in the neighboring cells; $\boldsymbol{C_0}, \boldsymbol{C_1}, \boldsymbol{C_2}, \boldsymbol{C_3}, \boldsymbol{C_n}$ represent the coefficients that connect each cell value to each of its neighboring cell values; and S denotes the source term. These algebraic equations are solved for the field variables T, u, v, w and density ρ. This implies that if n cells are present in the domain, then a total of 5n equations are solved.

5.4 Turbulence Modeling

Turbulent flow is defined as a flow regime characterized by irregular fluctuations in all directions and infinite number of degrees of freedom unlike laminar flow which is smooth and streamlined. The flow is described as three dimensional with rapid changes in velocity and pressure. Flows at larger Reynolds number (more than a few thousand) are generally considered turbulent while those with a lower Reynolds number are considered laminar. 6SigmaET® uses K-Epsilon turbulence model.

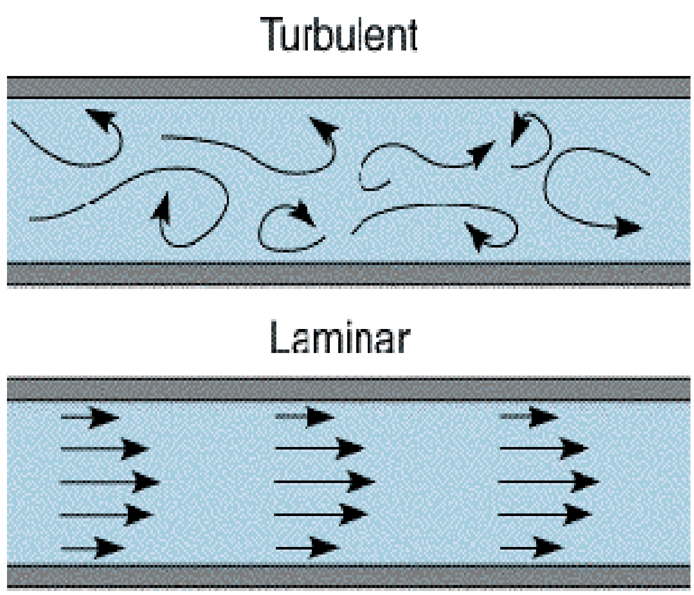

Figure 29 Graphical representation of laminar vs turbulent flow [24]

5.4.1 K-Epsilon Turbulence Model

K-Epsilon turbulence model is also commonly known as two equation model and is widely used for turbulent flow modeling. This model solves using two variables; the kinetic energy of turbulence (k) and the dissipation rate of kinetic energy of turbulence (ε) [25]. The two equation model computes viscosity depending on the grid cells rather than calculating the viscosity due to the walls. The K-Epsilon model is applicable for problems with thin shear layers and recirculating flows [25]. Two transport equations namely kinetic energy of turbulence (k) and dissipation rate of kinetic energy of turbulence are solved [25].

The following are the transport equations: [26]

$$\frac{\partial(\rho k)}{\partial t}+\frac{\partial \rho k u_i}{\partial x_i}=\frac{\partial}{\partial x_i}\left[\left(\mu+\frac{\mu_t}{\sigma_k}\right)\frac{\partial k}{\partial x_i}\right]+G_k+G_b-\rho\varepsilon$$

$$\frac{\partial(\rho \varepsilon)}{\partial t}+\frac{\partial \rho \varepsilon u_i}{\partial x_i}=\frac{\partial}{\partial x_i}\left[\left(\mu+\frac{\mu_t}{\sigma_k}\right)\frac{\partial \varepsilon}{\partial x_i}\right]+C_{1S}\frac{\varepsilon}{k}(G_k+C_{3S}G_b)-C_{2S}\rho\frac{\varepsilon^2}{k}$$

5.5 Grid Constraints and Meshing

Grid constraints are used for specifying minimum and maximum number of cells across the geometry. As discussed before, 6SigmaET® uses a Cartesian grid and object based gridding- pre-defined gridding rules which automatically decide the best grid for the simulation [22].

5.6 Objects

6SigmaET® uses the nomenclature used in the electronics industry. The entities in 6sigmaET® are parametrically defined and know their function and behavior, which makes the model easier to build and analyze. Instead of using a solid block for representing simple objects in space 6SigmaET® uses objects like chassis, PCB, chip socket, capacitors, Power supply unit etc., with predefined properties like Material properties and thermal properties including surface properties and can be modifies based on our requirement.

5.6.1 Test Chamber

A Test Chamber is a type of pseudo wind tunnel where you are able to set up a model and structure the airflow across it in a number of different ways. Test chamber encloses the chassis of the system. The required environment can be attached to test chamber sides or we may prescribe a flow through the sides. In this case, the left, right and bottom sides are specified as wall type.

5.6.2 Chassis

The Chassis object is the overall casing for the equipment, a default model is created with four sides, a Top and a Bottom, measuring 440mm (X) by 500mm (Z) and 1U (Y) in height. All that is necessary is for the user to adjust the size and shape of the Chassis using the data defined in the properties box and change the units of measure to our preferred system [27]. This object is a hollow cuboid with six sides that can be used to represent the outer shell of a server system. All the other components can be inserted within the chassis object. Each side of the object can be assigned different material, thickness and environment. Thermal and surface properties are automatically assigned based on the material selected. Thickness of the enclosure chassis can be specified and can be specified as thick or thin. The chassis object is commonly used for modeling data centers, racks and servers. Everything directly attached to the Chassis is organized under the Chassis node and consists of:

Cooling - consists of Fans, Blowers and Heat sinks

Electronics - consists of all Disk Drives and Bays, PCBs and the Components mounted on them, (including all of their associated hardware).

Fluid Cooling - includes any internal Ducting for a Fluid Cooling System and associated Pumps if they are internally mounted.

Obstructions - these would be used to model non heat producing items such as internal ironmongery, DIP switches, crystals, and various battery types etc. and heat producing items such as transformers, large chokes and solid state relays etc.

Power - consists of simple Power Supplies and their attached Fans.

Sensors - consists of only the Sensors attached to the Chassis. As Sensors can be attached to many different objects, those Sensors will be shown in the Model Tree under the object to which it is attached.

Sides - are the sides of the Chassis.

Sub Chassis - consists of any Sub chassis which is attached to the Chassis [27].

5.6.3 PCB

Printed circuit board, (PCB) is sheets of copper that is laminated onto a non-conductive substrate. They are processed to form a conductive path leaving other areas non-conductive. PCB is used to support components and connect them using the conductive tracks. In 6SigmaET®, PCB's are used to represent the motherboard housing the electronics of the server.

5.6.4 Sensors

Sensors represent the measurement devices that gather data about the environment and attached to a selected object for control. Sensors can be anywhere located within the solution domain for various objects. This includes chassis, PCB's, components, and vents. They are used for monitoring critical regions to record the temperature, pressure and velocity. For example, sensors can be used for recording server inlet and exhaust temperatures. These sensors help record data at required region of interest.

5.6.5 Fans

Fans are devices which are used for cooling electronic equipment by creating air to flow through the device. Fans create air flow by converting the torque supplied to the propeller shaft to impart kinetic energy to the air flowing across the fan rotor. In doing so, these devices also increase the static pressure across the fan rotor.

The most commonly used fans in cooling applications are axial flow. Axial flow fans deliver air flow in the direction parallel to the fan blade axis. These fans can deliver very high flow rates. They produce air flows with high volume and low pressure. They are used for cooling IT equipment and several other electronic devices. Axial fans can be classified into propeller fans, tube-axial fans and vane-axial fans [28].

5.7 PAC

The PAC in 6SigmaET® stands for parameterize, analyze and compare is used for performing parametric analysis for alternative cases. It allows us to vary numbers of input conditions and help to study corresponding outputs by selecting the required parameter using configure input parameters tool. It reduces the time taken to compare models by compiling the output in a single window. A mesh sensitivity analysis can also be performed by varying the number of grid elements and performing a parametric study to obtain solutions to all trials simultaneously. Parametric analysis can be performed for fans with different fan speeds, flow rate, heat sink fin thickness, and fin count. Similarly, outputs that are required can be selected in the configure output parameters tool. Specific monitor points and regions can be selected to determine minimum, maximum and mean temperature, pressure and velocity immediately.

CHAPTER 6

CFD MODELING AND FLOW ANALYSIS

6.1 Detailed Modeling of Server

Server modeling was done using 6SigmaET®. It is highly difficult to include all the components on the motherboard as they might not contribute to the system resistance. Certain components heat dissipation would negligible when compared to the total heat generated by the server. To develop a detailed model, major flow restricting and heat generating components were chosen. This was done based on the geometry and maximum Thermal Design Power (TDP) of each component.

Table 3 List of TDP of major components

Device	Reference Designator	TDP (W)
Processors	CPU0	95
	CPU1	95
DIMMS	A0	0.81
	A3	0.81
	A6	0.81
	B0	0.81
	B3	0.81
	B6	0.81
Chipsets	ICH	4.3
	IOH	27.1
Fans	Fan1	0.7-5.64
	Fan2	0.7-5.64
	Fan3	0.7-5.64
	Fan4	0.7-5.64
Power Supply	PS	4.5% of server power
Hard Drives	HDD	7.8

The modeling of server was carried out into two separate parts, Server motherboard modeling and Power supply unit modeling. The primary reason to model the Power supply unit separately as it has a dense configuration with lot of components and has a separate cooling fan powered by the PSU which does not vary with CPU loading. Initially a detailed model of the complete server was developed without the PSU.

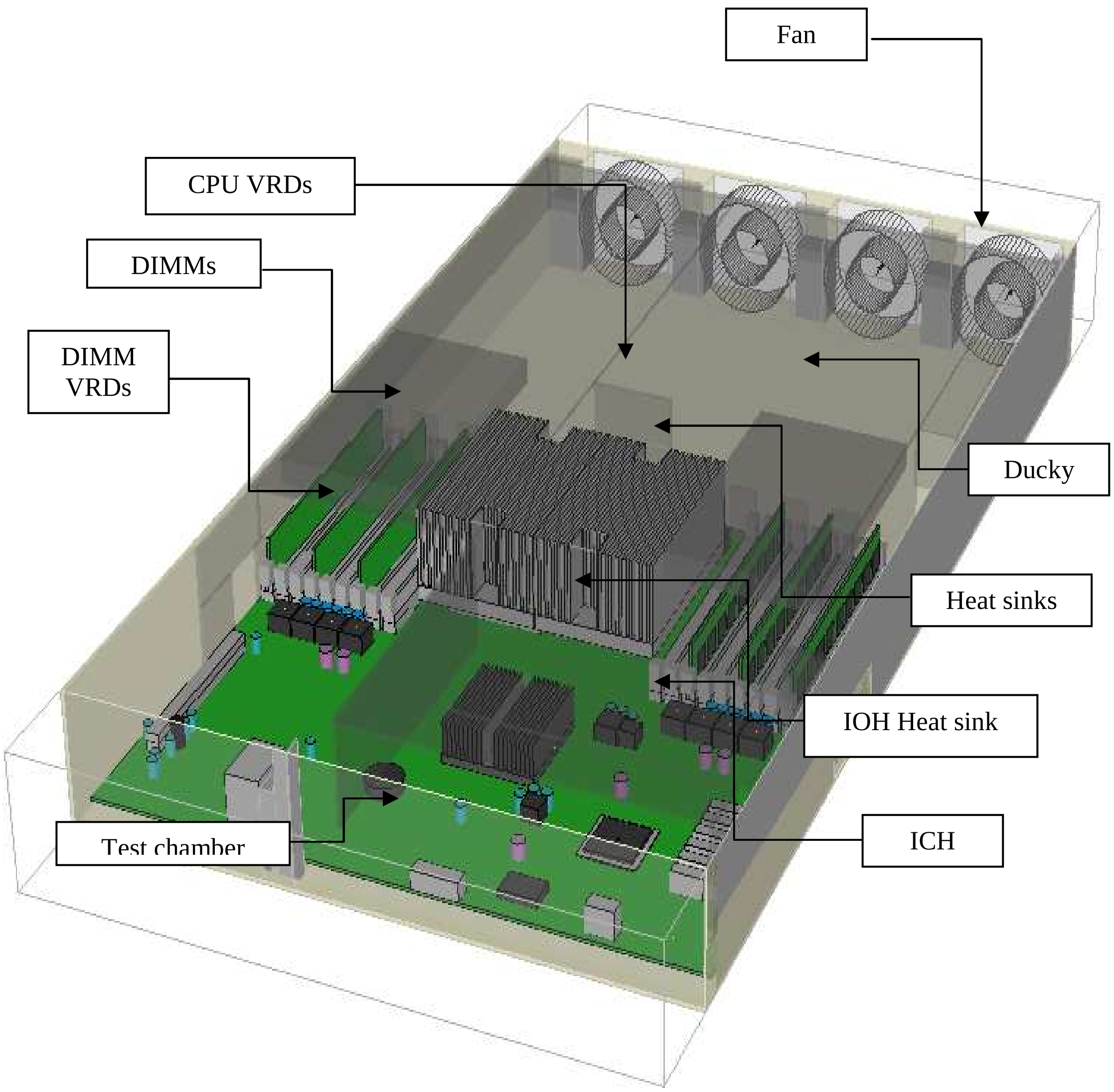

Figure 30 Detailed server model-Motherboard part

The air flows through the server through the front side and exits through the rear. A test chamber was created measuring the same dimensions of the server chassis. This test chamber serves as a virtual environment replicating the experimental setup. The server fans, VRDs, capacitors, DIMM slots, and chipsets are modeled as intelligent parts.

6.1.1 Heat Sink Modeling

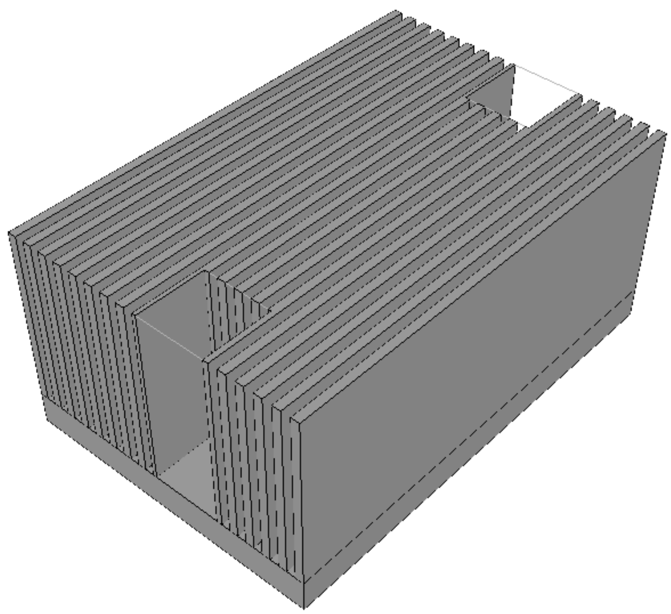

Figure 31 Detailed Heat sink model

The heat sink model was created in a detailed manner which includes minute geometric features. The heat sinks were tested on air flow bench and its system resistance was calculated and the model was also simulated in 6SigmaET® to verify modeling accuracy.

6.1.2 Server Ducky Modeling

The server ducky serves as a duct to channelize the flow through major heat generating components like heat sinks and VRDs. The ducky was model as a solid obstruction. It helps the air to flow through the components in a confined path maximizing the convection rate. It also acts as a lid to cover the top side of the chassis.

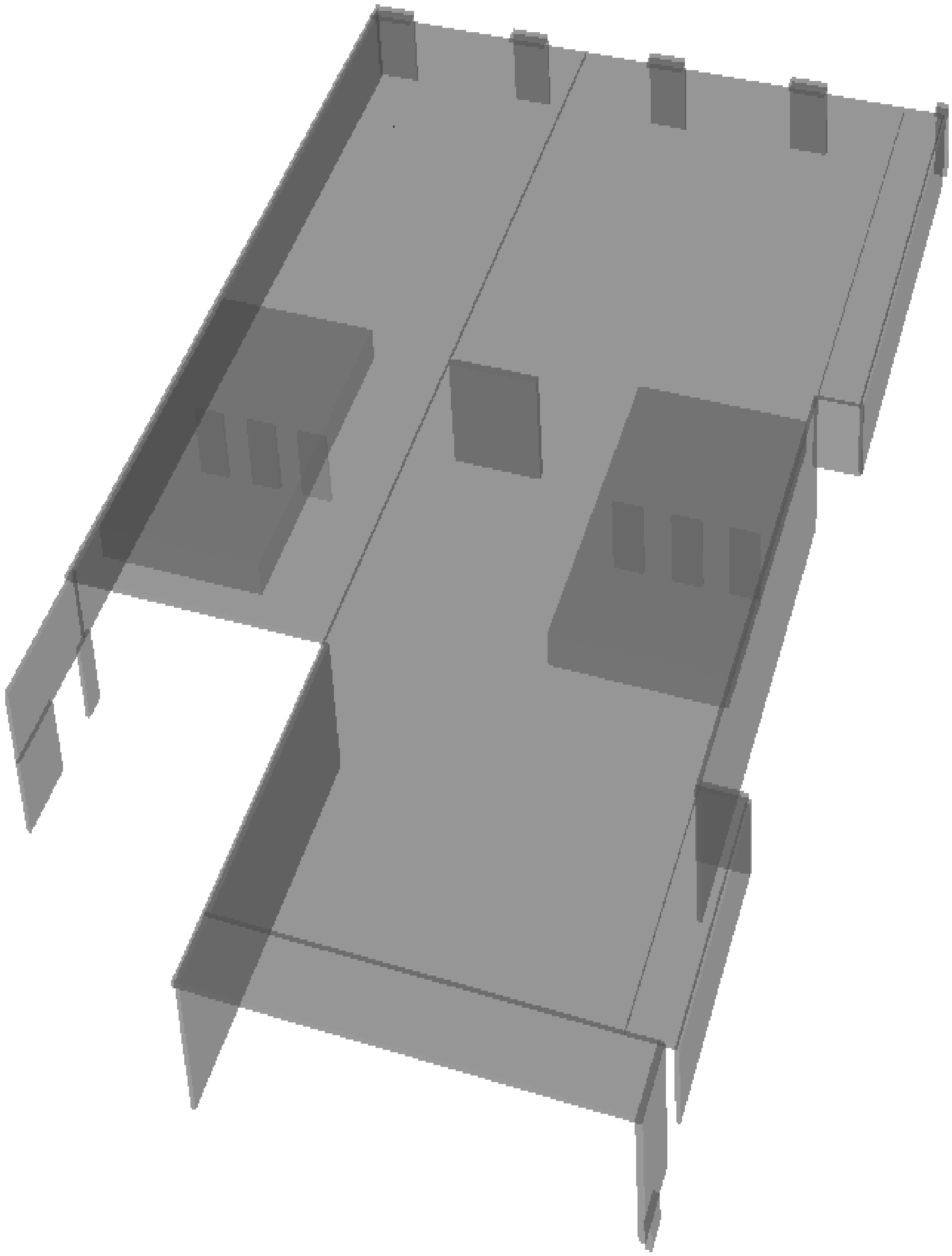

Figure 32 Server ducky

6.2 Power Supply Unit Modeling

The PSU model was modeled in PRO-E and was imported using 6Sigma CAD. The model was created as individual components and assembled together. The material properties were specified to individual components. The dimensions of the PSU are 120x63x220mm. The power supply unit components were measured individually and modeled. The power supply unit was considered as a sub assembly; hence flow analysis had to be performed separately. The PSU has capability of working with both AC supply and DC supply. Hence, the PSU is divided into two sections. The AC side of the PSU has a folded plastic cover which helps to channelize the flow through the AC side and it also to prevent mixing of air from either side.

Figure 33 Power supply unit

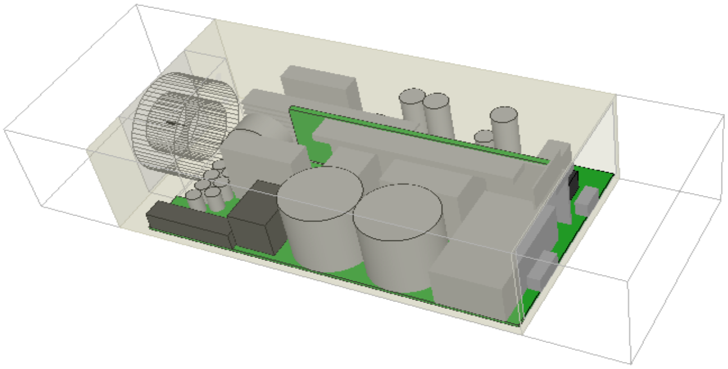

Figure 34 Detailed CFD PSU model

6.3 Experimental Results

6.3.1 Experimental System Impedance of Server

As mentioned earlier, the system impedance of server with different setups were measured to validate the CFD model. The server was setup in an airflow test chamber and a fixed flow rate was supplied through the chamber into the server and static pressure was measured. This was performed with different flow rates. The graph below gives us a clear comparison of static pressure variation between different server setups.

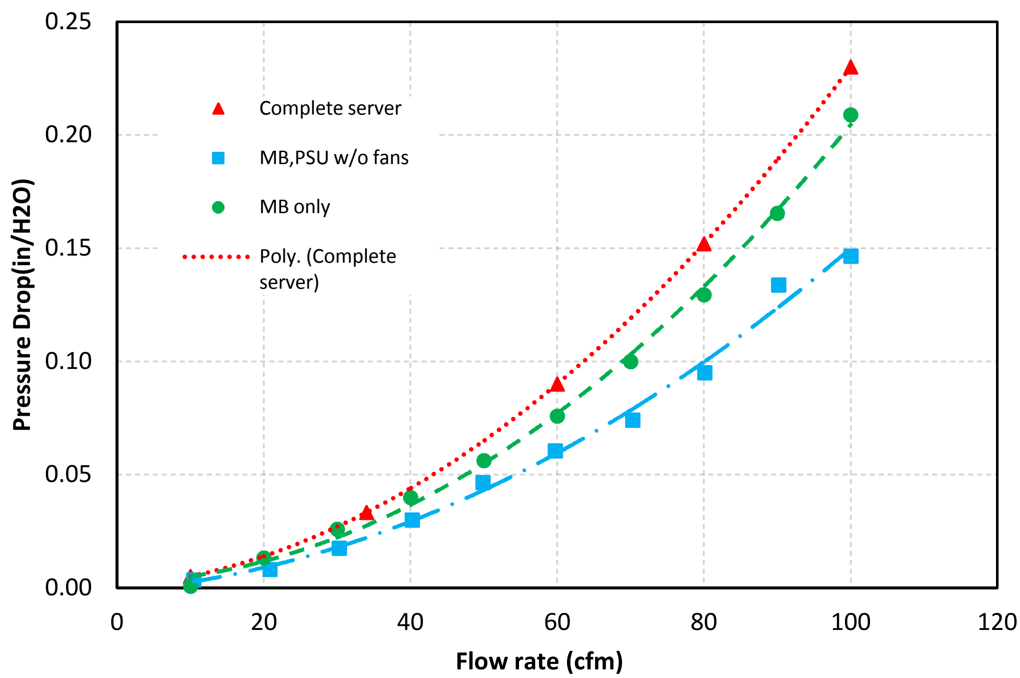

Figure 35 Experimental static pressure measurements

6.3.2 Experimental Flow rate through server Motherboard Part

The server flow rate was measured by powering the fans separately using a DC power supply and a function generator. The duty cycle was varied to vary the fan speed thereby varying the flow rate through the airflow chamber. PSU was blocked and measurements were taken for the server motherboard part only. This gives us a clear picture on the flow rate only through the motherboard.

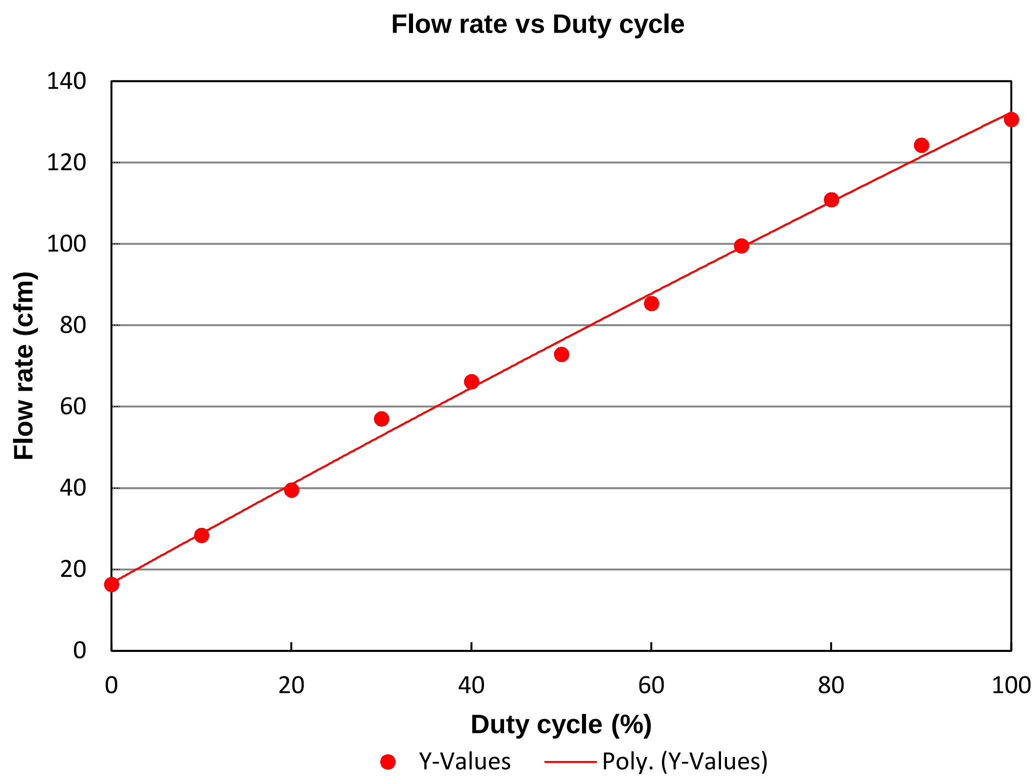

Figure 36 Experimental flow rate for various % duty cycles

Table 4 Experimental flow rate fan speeds for various % duty cycles

PWM	Fan speed	Flow rate
%	rpm	cfm
100	8978	130.62
90	8426	124.29
80	7700	110.89
70	6935	99.55
60	6137	85.39
50	5350	72.88
40	4574	66.17
30	3802	57.03
20	3008	39.51
10	2238	28.38
0	1535	16.33

6.3.3 Experimental System Impedance of Heat Sink

The below table consists of static pressure drop values for different flow rate through the heat sink.

Table 5 Experimental static pressure drop across heat sinks

Experimental Values	
Flow rate (cfm)	Static Pressure drop (inH2O)
4	0.0191
8	0.049
12	0.0888

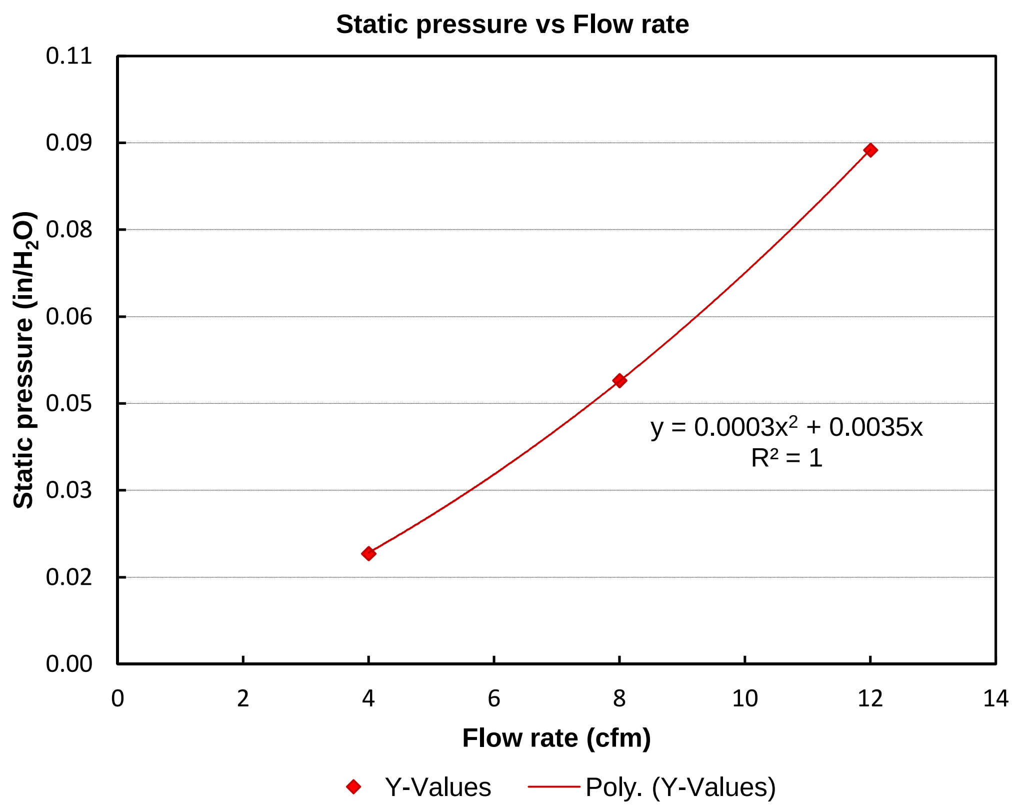

Figure 37 Graph representing the static pressure drop across the heat sink

6.3.4 Experimental System Impedance of PSU

The table below consists of static pressure drop across the PSU without fans.

Table 6 Experimental PSU static pressure drop

Experimental values	
Flow rate (cfm)	Static Pressure drop (in/H_2O)
4	0.00447
8	0.01700
15	0.05829
20	0.10288
30	0.22980

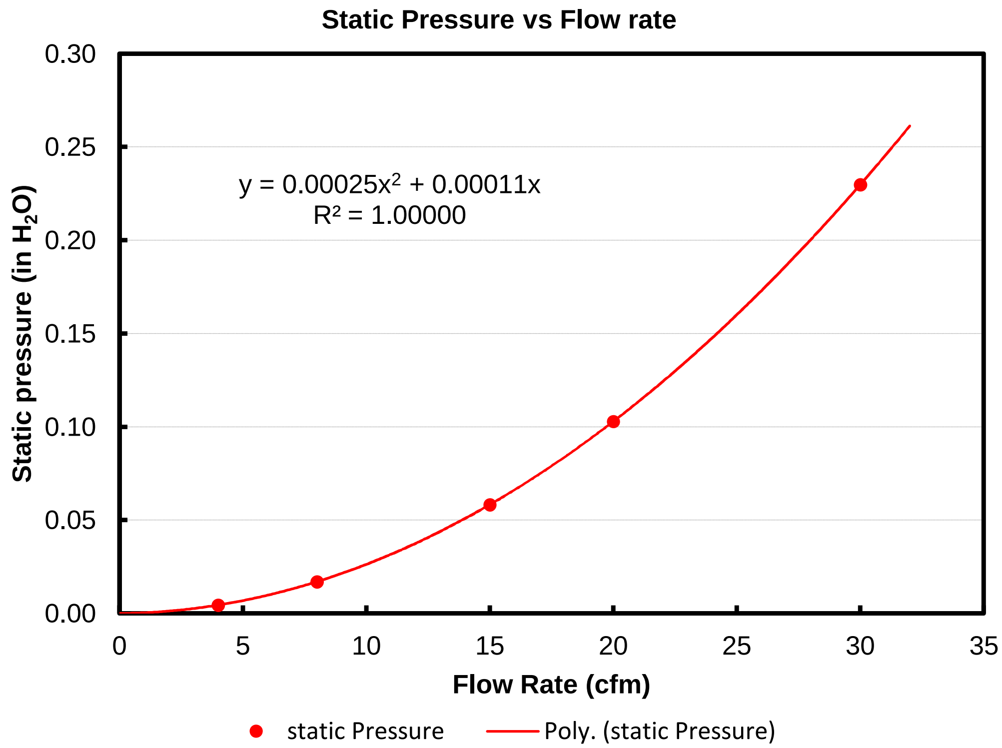

Figure 38 Graph representing the static pressure drop across the PSU

6.3.5 Experimental Flow Rate through PSU

The below table consists of static pressure drop values for different flow rate through the PSU.

Table 7 Experimental flow rate fan speeds for various % duty cycles

PWM	Fan speed	Flow rate
%	rpm	cfm
30	1982	8.97
40	2713	11.54
50	3408	13.98
60	4085	16.36
70	4720	18.59
80	5312	20.67
99.9	6384	24.44

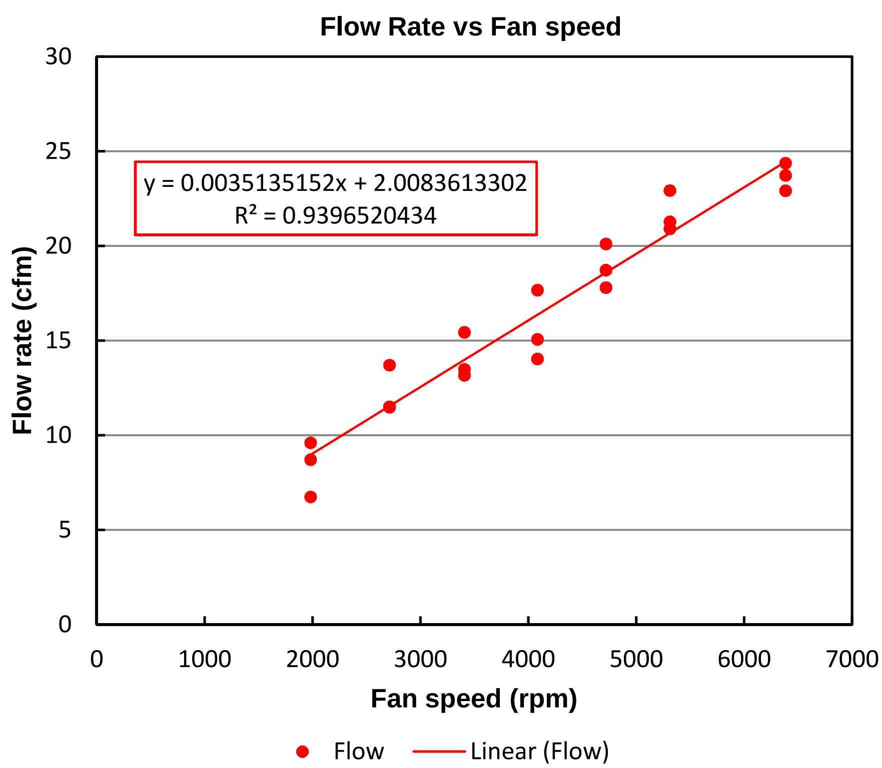

Figure 39 Graph representing fan flow rate through PSU

CHAPTER 7

COMPARISON OF RESULTS AND CONCLUSION

7.1 Mesh Sensitivity Analysis

Mesh sensitivity analysis was performed to ensure the results are grid size and count independent. This is a important procees in computaional simulation as it determines the accuracy of the resultsThe cell count was varied from 2.5 million to 50 million. It was observerd that the pressure incresed with increse in cellcount and steady out after reaching 17 million cells. The termination factor was reduced to 0.1 to ensure the inflow and the outflow through the system is equal. The same procedure is followed for the PSU model and the solution was observed to steady after grid count was increased to 15 million cells. The aspect ration was also maintained below 12 in both the cases.

In case of flow rate simulations, the flow relaxtion rate was changed from the default value of 0.5 to a point were the fan flow rate values stablizes wiithout any rapid oscilations in the mointoring points or the residuals. It flow rate relaxation values vary for different models.

Table 8 Mesh sensitivity analysis for server motherboard part

Cell count	Pressure(Pa)
2966432	9.85
6671160	11.63
11833875	12.73
17031904	12.95
26487054	13.04
53000000	13.05

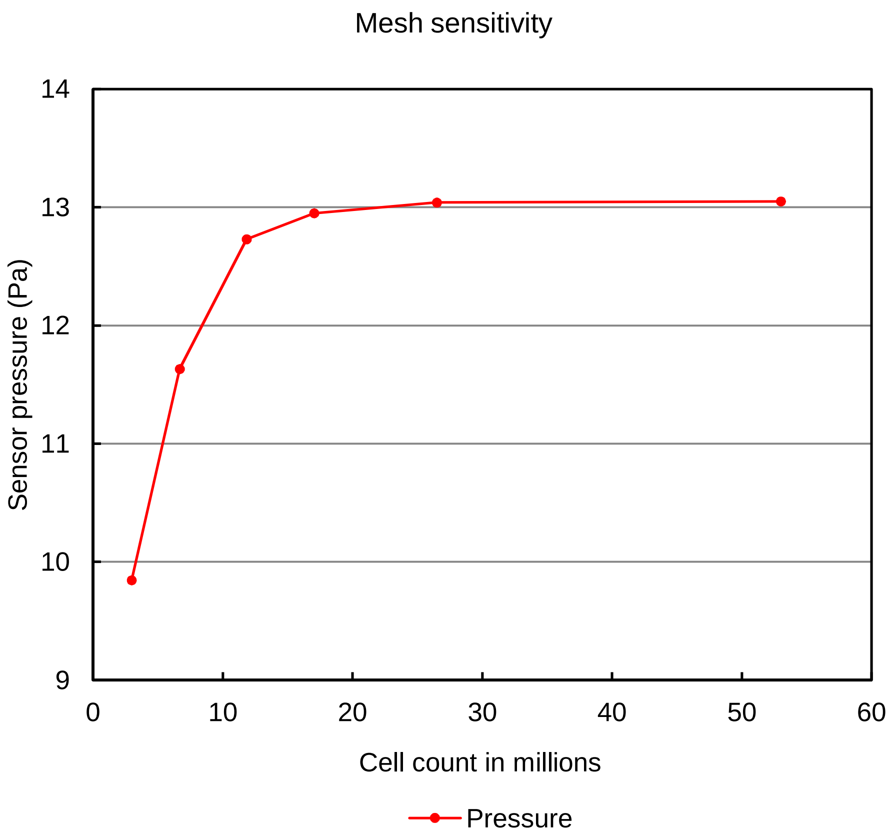

Figure 40 Mesh sensitivity analysis for server motherboard part

Table 9 Mesh sensitivity analysis for PSU

Cell Count	Pressure(Pa)
1442048	12.7
3995952	13.2
7393200	13.4
15752364	13.7
30990938	13.8
59324560	13.8

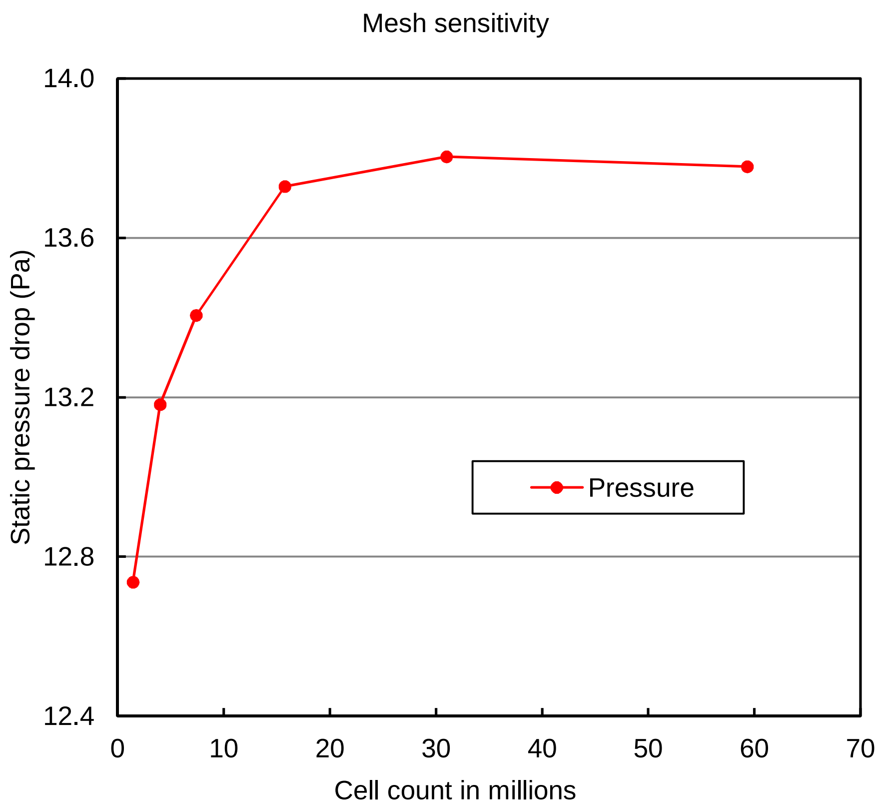

Figure 41 Mesh sensitivity analysis for PSU

7.2 Comparison of Experiment and CFD Server Motherboard Part System Impedance

Experimental results of system impedance of server motherboard part was compared with the CFD simulation results. The experiment was carried out by blocking the inlet to the PSU unit at the inlet before placing it into the air flow chamber. The experiment was carried out for different flow rate by varying the counter blower.

Similarly, the simulation was carried out with the motherboard only model excludimg the PSU. The simulation was also carried out for different flow rate and compared with the experimental values.

Table 10 Comparison between experimental and computaional system impedance

Flow rate (cfm)	Experimental (in/H_2O)	CFD (in/H_2O)	%Error
20	0.011	0.012	7.9
40	0.040	0.036	10.3
50	0.058	0.052	10.0
60	0.078	0.071	9.6
80	0.119	0.114	4.2
90	0.148	0.144	2.9
100	0.181	0.172	5.0

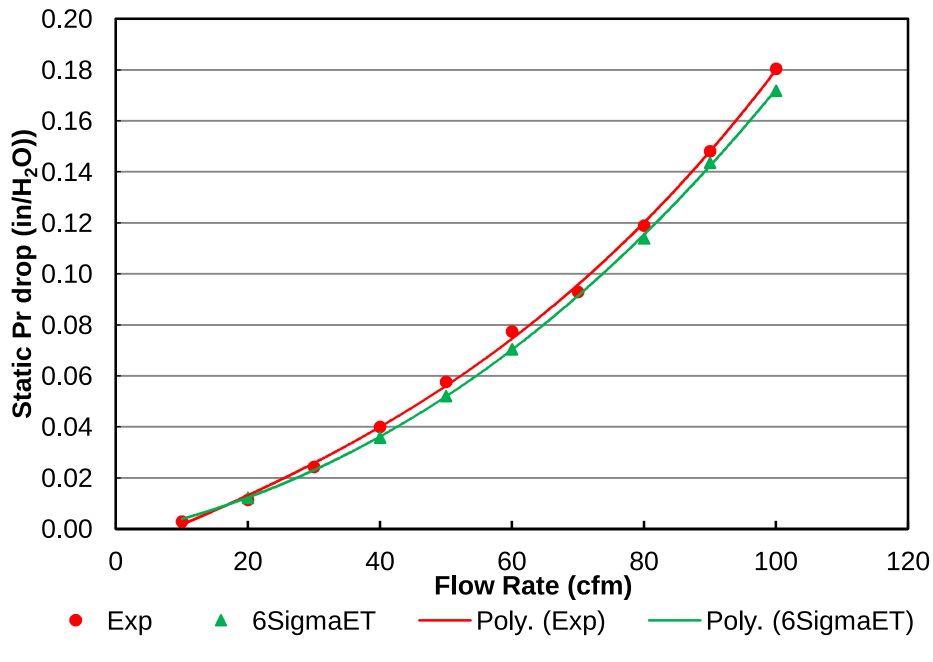

Figure 42 Comparison of experimental and compuational system impedance of the server motherboard part

7.3 Comparison of Experimental and CFD Fan Flow Rate through Server Motherboard

The server fans were externally controlled and powered to run the fans at specific speed and flow rate determined experimentally using airflow chamber. The PSU was blocked at the inlet before testing it in the chamber to avoid any airflow through it. The simulation was carried out with server fans installed to the model and at different fan speeds. The flow rate measured at the inlet and the outlet of the server.

Table 11 Comaprison between experimental and computational server fan flow rates

% Duty Cycle	Fan Speed (rpm)	Volumetric Flow rate (cfm)		% Error absolute value
		Experimental	CFD	
100	8978	130.6	133.9	2.5
90	8426	124.3	124.7	0.3
80	7700	110.9	113.0	1.9
70	6935	99.6	100.8	1.3
60	6137	85.4	89.5	4.9
50	5350	72.9	77.0	5.6
40	4574	66.2	63.2	4.5
30	3802	57.0	51.8	9.2
20	3008	39.5	39.1	0.9
10	2238	28.4	28.0	1.4
0	1535	16.3	18.0	10.2

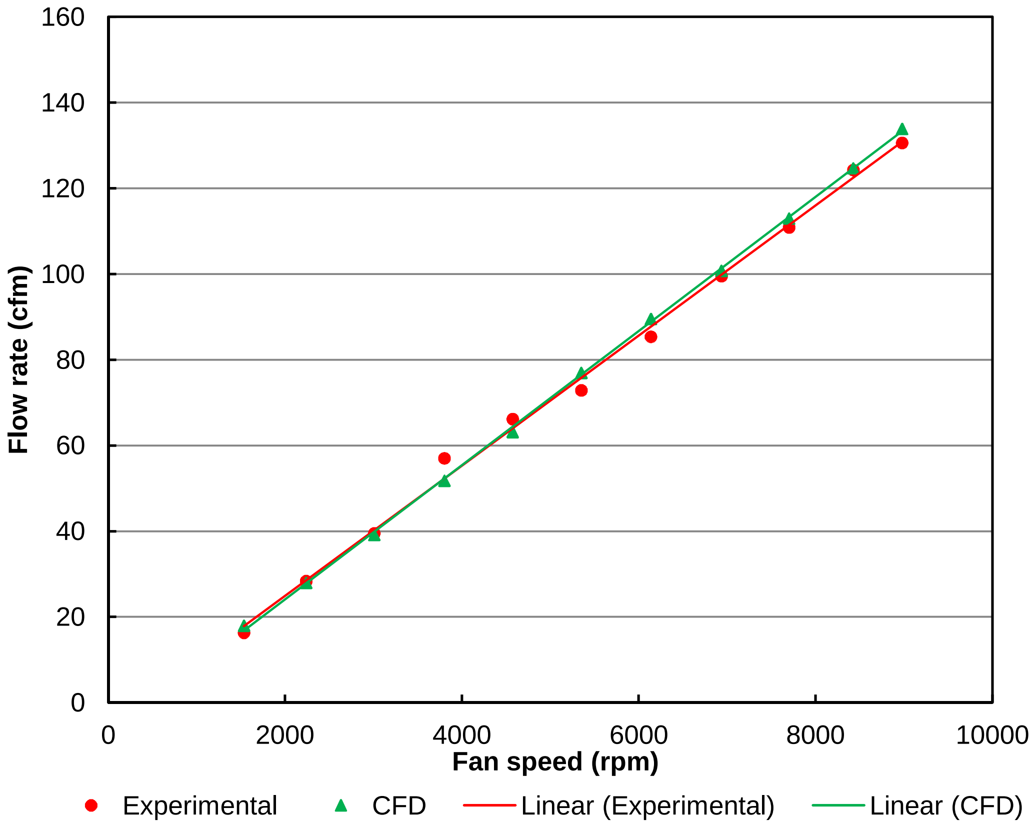

Figure 43 Comparison of experimental and compuational serverfan flow rates

7.4 Comparison Of Experimental and CFD System Impedance of PSU

Experimental results of system impedance of server power supply unit was compared with the CFD simulation results. The experiment was carried out with only the PSU unit placed at the inlet of the air flow chamber. The experiment was carried out for different flow rate by varying the counter blower.

Similarly, the simulation was carried out with the PSU model with fans uninstalled from the model. The simulation was also carried out for different flow rate and compared with the experimental values.

Table 12 Comparison of experimental and computaional PSU system impedance

Experimental		CFD	
Fl. Rate	St. Press (in/H_2O)	St. Press (in/H_2O)	%Error
4	0.0044	0.0042	4
8	0.0170	0.0171	1
15	0.0583	0.0552	5
20	0.1029	0.0947	8
30	0.2298	0.2057	10

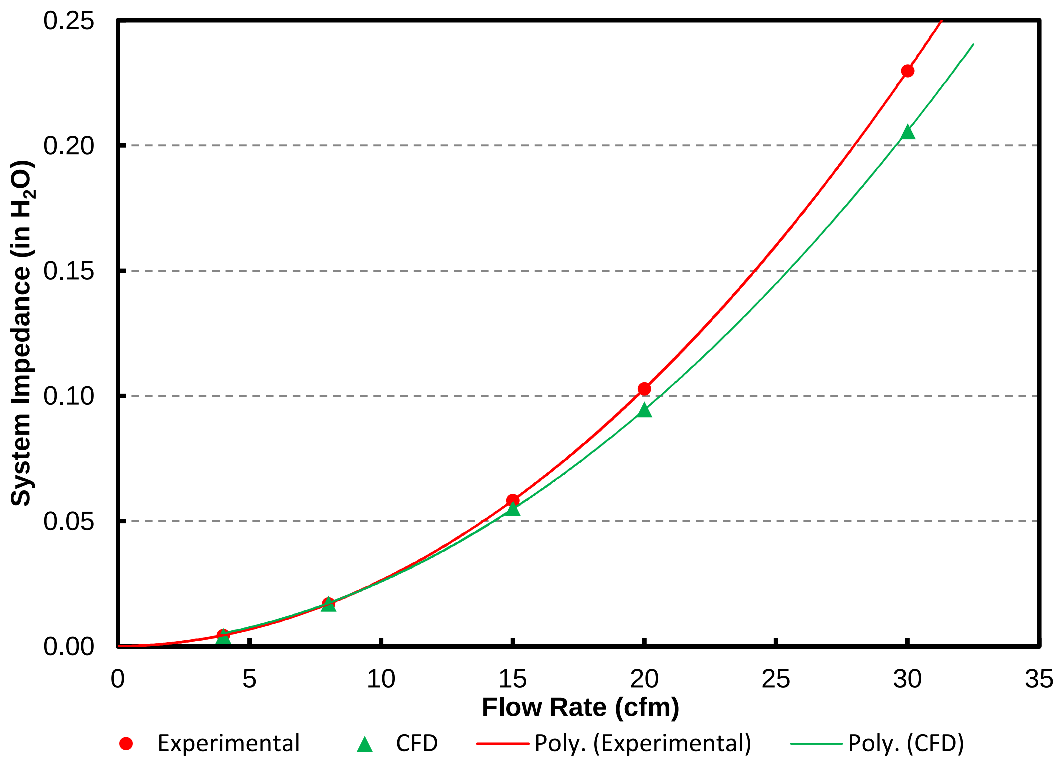

Figure 44 Experimental and computational comparison of PSU system impedance

7.5 Comparison of Experimental and CFD Fan Flow Rate through PSU

The server fans were externally controlled and powered to run the PSU fans at specific speed and flow rate experimentally determined using airflow chamber. The simulation was carried out with PSU fans installed to the model and at different fan speeds. The flow rate measured at the inlet and the outlet of the server.

Table 13 Comaprison between experimental and computational fan flow rates through PSU

Fan speed (rpm)	Flow Rate (cfm)		%Error
	Experimental	CFD	
6000	23.09	25.48	10.4
5000	19.58	21.19	8.2
4000	16.06	16.80	4.6
3000	12.55	12.46	0.7
2000	9.04	8.14	9.9

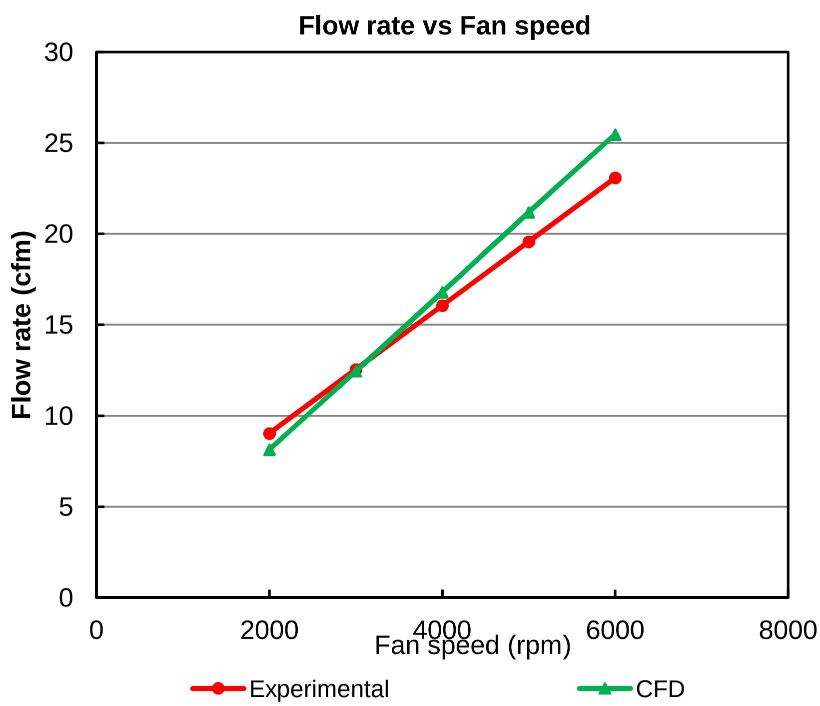

Figure 45 Experimental and computational comparison of PSU fan flow rate

7.6 Conclusion

The comparison between experimental and computational results for system impedance of both the server motherboard part and power supply unit has been listed above. From the comparison we can observe that the error percentage between experimental and computational system impedance results for server motherboard part was as a minimum of 4.6% to 10.3%. For flow rates, the minimum and maximum error percentage between experimental and computational values is 0.3% to 10.2%. Comparing the experimental and computational system impedance results for PSU was observed to be a minimum of 1% to a maximum of 10%. As the simulation results are within 10% error form the experimental results, we can conclude that the CFD model is accurate and is experimentally validated

REFERENCES

1. Steven Pelleyy David Meisnery Thomas F. Wenischy James W. VanGilderz, “Understanding and Abstracting Total Data Center Power”.
2. “Best Practices Guide for Energy-Efficient Data Center Design”, http://www1.eere.energy.gov/femp/pdfs/eedatacenterbestpractices.pdf, 2011.
3. http://nsidc.org/about/green-data-center/project.html
4. http://emersonnetworkpower.com/en-US/Services/DCN/Pages/default.aspx
5. http://en.wikipedia.org/wiki/File:IBM_HS20_blade_server.jpg
6. http://www.ehow.com/facts_7550954_difference-between-rack-blade-server.html
7. “Open compute project Intel motherboard hardware 1.0”, http://opencompute.org/wp/wp-content/uploads/2011/07/Server-Intel-Motherboard-Specifications-v1.pdf.
8. http://www.datacenterknowledge.com/archives/2011/04/08/roundup-is-open-compute-a-game-changer/
9. “Development of an Experimentally-Validated Compact Model of a Server Rack”, Graham Nelson, Georgia Institute of Technology, December 2007.
10. http://opencompute.org/projects/intel-motherboard/
11. “Open compute project server chassis and triplet hardware 1.0”, http://opencompute.org/wp/wp-content/uploads/2011/07/Server-Chassis-Specifications.pdf
12. http://www.delta.com.tw/product/cp/dcfans/download/pdf/QFR/QFR60x60x25.4mm.pdf
13. “Open compute project 450W power supply”, http://opencompute.org/wp/wp-content/uploads/2011/07/Server-Power-Supply-Specifications.pdf
14. ebm-papst Inc., “Air Flow Performance and Speed at a Glance”, www.ebmpapst.us.

15. http://www.setra.com/ProductDetails/264_HVAC.htm
16. http://www.fantester.com/
17. http://fab.cba.mit.edu/classes/MIT/961.04/topics/pwm.pdf
18. Suhas V Patankar, “Computational fluid dynamics: Engineering Analysis and Application”.
19. John D. Anderson, Jr., “Computational fluid dynamics, The Basics with Applications”.
20. S.V. Patankar, “Numerical Heat Transfer and Fluid Flow”, New York, 1980.
21. Robert Eymard, Thierry Gallou¨et and Rapha`ele Herbin, “Finite Volume Methods”, October 2006.
22. http://www.futurefacilities.com/software/et/6SigmaET.php
23. André Bakker, “Applied Computational Fluid Dynamics”, http://www.bakker.org
24. http://blog.nialbarker.com/252/slow_is_faster
25. B.E. Launder and D.B. Spalding, “The Numerical Computation of Turbulent Flows”, Appendix D of Computer Methods in Applied Mechanics and Engineering, 1974, pp. 269-289.
26. K.K. Dhinsa, C.J. Bailey, and K.A. Pericleous, "Low Reynolds Number Turbulence Models for Accurate Thermal Simulations of Electronic Components," Proc of the International Conference on Thermal and Mechanical Simulation and Experiments in Micro-Electronics and Micro-Systems, EuroSimE 2004.
27. http://downloads.futurefacilities.com/Downloads/CurrentRelease/6SigmaET-Guide-R7.pdf
28. Energy Efficiency Guide for Industry in Asia, “Electrical Energy Equipment: Fans and Blowers”, UNEP, 2006, www.energyefficiencyasia.org.

BIOGRAPHICAL INFORMATION

Vijayalayan Pandiyan received his Bachelor's Degree in Mechanical Engineering from Velammal Engineering College, Chennai, India in May 2008. He completed his Master of Science degree in Mechanical Engineering at the University of Texas at Arlington in December 2012.

Vijayalayan Pandiyan has been involved in a number of projects ranging from the device level to the rack/room level. His research areas include impact of higher inlet temperature on servers, testing of heat sinks, rack and room level CFD modeling.

He has handled a number of projects such as analysis of temperature on servers at various utilizations, fan characterization to determine fan curves, vapor chamber heat sink and conventional heat sink comparison, 3D CAD modeling of server and power supply units using PRO-E, Thermal and mechanical analysis of different types of TIMs on a flip chip package, Impact of containment and plenum height on data center. He has worked on several industry projects during his research at the UTA.